From THE DEPARTMENT OF CLINICAL NEUROSCIENCE
Karolinska Institutet, Stockholm, Sweden

PHARMACOLOGICAL PROPERTIES OF RADIOTRACERS THAT MEASURE P-GLYCOPROTEIN FUNCTION AND DENSITY

Pavitra Kannan

Karolinska Institutet

Stockholm 2012

Cover Illustration:

Pictured is a PET image of a human (left side of figure) showing the upper-body distribution of the radiotracer [^{11}C]*N-desmethyl*-loperamide, which is a P-glycoprotein substrate that has irreversible accumulation in the kidneys and spleen. As described in this thesis, the irreversible accumulation of this tracer is a result of its trapping in acidic organelles known as lysosomes (shown in red in the human cells; right side of figure) and is a mechanism that amplifies the PET signal. Image courtesy of Kyle Brimacombe, Matthew Hall, William Kreisl, and Jeih-San Liow.

All previously published papers were reproduced with permission from the publisher.

Published by Karolinska Institutet. Printed by Larserics Digital Print AB.

© Pavitra Kannan, 2012
ISBN 978-91-7457-645-0

To my sister.

Le vrai est trop simple; il faut y arriver toujours par le compliqué.
[*The truth is too simple; one must always find it through the complicated.*]

-Amantine Lucile Aurore Dupin

ABSTRACT

Energy-dependent transporters of the ATP-binding cassette (ABC) family regulate the movement of molecules across cellular membranes. Several of these transporters are expressed in the endothelial cells of brain microvessels (blood-brain barrier) to protect brain tissue from exposure to toxins in the blood. Three of the most common ABC transporters at the blood-brain barrier are P-glycoprotein (P-gp), breast cancer resistance protein (BCRP), and multidrug resistance protein 1 (MRP1). Changes in P-gp function and density are hypothesized to play a role in neurological disorders, mediating drug-resistant epilepsy, drug effectiveness against HIV infection of the brain, and Alzheimer disease. Therefore, to measure P-gp function and density in vivo, substrates (which are transported by P-gp) and inhibitors (which bind to P-gp) have been radiolabeled for use in the nuclear imaging technique positron emission tomography (PET). For accurate quantification, radiotracers must be selective for P-gp and have high signal strength. The purpose of this thesis was to evaluate whether two radiotracers that are used to image P-gp function and density fulfill these properties.

The selectivity and signal strength of the P-gp substrate *N-desmethyl*-loperamide (dLop) and the P-gp inhibitor tariquidar were assessed using pharmacology assays in human cell lines and post-mortem mouse brains, and using PET imaging in transgenic mice and healthy humans. We found that the radiotracer [^{11}C]dLop is selective as a substrate for P-gp among the three major ABC transporters of the blood-brain barrier because accumulation of [^{3}H]dLop was lowest in cells expressing P-gp, and the uptake of [^{11}C]dLop was highest in brains of mice lacking P-gp. In addition to being selective, dLop is ionically trapped in acidic lysosomes; [^{3}H]dLop accumulation decreased by $\geq$ 50% in human cells pretreated with compounds that raise lysosomal pH. This irreversible trapping mechanism of [^{11}C]dLop amplifies the measured PET signal because radioactivity accumulates over time. However, the P-gp inhibitor tariquidar competes with dLop for lysosomal accumulation because it decreased the accumulation of [^{3}H]dLop by $\geq$ 50% in human cells and that of [^{11}C]dLop by $\geq$ 35-40% in lysosome-rich organs of P-gp knockout mice and healthy humans; competition was not observed in the brain. The lysosomal competition in the peripheral organs is problematic because tariquidar is used in combination with [^{11}C]dLop to measure P-gp function in vivo and suggests that these two compounds cannot be used together to measure P-gp function in the periphery.

We also found that tariquidar is not a specific inhibitor of P-gp; it is also a substrate and inhibitor of BCRP. At low concentrations, [^{3}H]tariquidar had highest accumulation in cells expressing P-gp and lowest accumulation in cells expressing BCRP, while at higher concentrations ($\geq$ 100 nM), tariquidar inhibited the function of both P-gp and BCRP. In addition to not being selective, [^{11}C]tariquidar has a low signal strength as a radiotracer because specific binding of [^{3}H]tariquidar to P-gp in post-mortem mouse brains was only 20-30% of the total signal.

In conclusion, the selectivity and high signal strength of the radiotracer [^{11}C]dLop allow it to selectively measure P-gp function at the blood-brain barrier and this radiotracer can be used to determine P-gp's role in neurological disorders. In contrast, the lack of selectivity and low signal strength of [^{11}C]tariquidar indicate that this inhibitor cannot measure P-gp density and that better inhibitor radiotracers are required.

RÉSUMÉ

Les transporteurs appartenant à la famille ATP Binding Cassette (ABC) contrôlent le mouvement des molécules à travers les membranes des cellules. Plusieurs de ces transporteurs se trouvent dans les cellules endothéliales des micro-vaisseaux cérébraux (la barrière hémato-encéphalique) afin de protéger le cerveau contre les toxines contenues dans le sang. Les trois principaux transporteurs ABC de cette barrière sont la P-glycoprotéine (P-gp), la BCRP et la MRP1. Parmi eux, les changements de fonction et de densité de la P-gp sont supposés jouer un rôle dans la résistance aux médicaments contre l'épilepsie, l'efficacité des médicaments contre l'infection cérébrale du VIH et de la maladie d'Alzheimer. Afin de quantifier la fonction et la densité de la P-gp in vivo, des substrats (transportés par la P-gp) et des inhibiteurs (qui s'attachent à la P-gp) ont été radiomarqués pour la tomographie par émission de positons (TEP), une méthode d'imagerie nucléaire. Or, pour une quantification précise de TEP, un radiotraceur doit à la fois être sélectif pour la P-gp et fournir un rapport signal/bruit élevé. L'objectif de cette thèse était donc d'évaluer si deux radiotraceurs, dont l'utilité est de mesurer la P-gp in vivo, satisfont ces deux propriétés.

Ces propriétés ont été évaluées pour le substrat *N-desmethyl*-loperamide (dLop) et l'inhibiteur tariquidar en utilisant les méthodes pharmacologiques dans des lignées cellulaires humaines et des cerveaux de souris post-mortem, ainsi qu'à partir de l'imagerie TEP chez les souris transgéniques et les humains. Nous avons constaté que le radiotraceur [^{11}C]dLop est sélectif comme substrat de la P-gp parmi les trois principaux transporteurs ABC ; la capture cellulaire de [^{3}H]dLop a été la plus faible dans la lignée exprimant la P-gp, tandis que la capture cérébrale de [^{11}C]dLop a été la plus forte chez la souris *knockout* pour la P-gp. De plus, le dLop est ioniquement piégé dans les lysosomes parce que la capture cellulaire de [^{3}H]dLop a été diminuée d'au moins 50% dans les lignées prétraitées des composés augmentant le pH lysosomal. Ce mécanisme irréversible du piégeage amplifie le signal mesuré par TEP parce que la radioactivité augmente avec le temps. Il a également été découvert que l'inhibiteur tariquidar a baissé de 50% l'accumulation de dLop dans les lignées cellulaires, et de 35 à 40% dans les organes riches en lysosomes chez les souris *knockout* pour la P-gp et les humains ; aucun effet n'a été mesuré au niveau du cerveau. Puisque le tariquidar est utilisé avec le [^{11}C]dLop pour mesurer la fonction de la P-gp, la concurrence entre les deux composés pour l'accumulation lysosomale signifie qu'ils ne peuvent pas être utilisés ensemble pour mesurer la fonction de la P-gp à la périphérie du corps.

Nous avons aussi constaté que le tariquidar n'est pas un inhibiteur spécifique de la P-gp ; il est aussi substrat et inhibiteur de la BCRP. Quand la concentration de [^{3}H]tariquidar était faible, sa capture cellulaire a été la plus forte dans la lignée exprimant la P-gp et la plus faible dans celle exprimant la BCRP. En revanche, dans le cas d'une concentration forte de [^{3}H]tariquidar, la fonction de la P-gp et de la BCRP a été inhibé. En outre, [^{11}C]tariquidar donne un faible rapport signal/bruit car le lien spécifique du tariquidar avec la P-gp dans les cerveaux de souris post-mortem n'a été que de 20 à 30% du signal total.

En conclusion, les deux propriétés – la sélectivité et le rapport élevé signal/bruit – confèrent un avantage au radiotraceur [^{11}C]dLop pour mesurer la fonction de la P-gp. Ce radiotraceur peut ainsi être utile pour déterminer le rôle de P-gp dans les maladies neurologiques. Par contre, la manque de sélectivité et le faible signal de [^{11}C]tariquidar indiquent que cet inhibiteur ne peut pas être utilisé pour mesurer la densité de la P-gp, et que de meilleurs inhibiteurs sont alors nécessaires.

LIST OF THESIS PUBLICATIONS

The following three papers are included after the summary chapter and are referred to by their roman numerals in the text. In addition, a review paper related to this thesis is included in the Appendix.

I. **Kannan P**, Brimacombe KR, Zoghbi SS, Liow JS, Morse C, Taku A, Pike VW, Halldin C, Innis RB, Gottesman MM, Hall MD. *N-desmethyl*-loperamide is selective for P-glycoprotein among three ATP-binding cassette transporters at the blood-brain barrier. *Drug Metab. Disp.* **38**, 917-22 (2010).

II. **Kannan P**, Brimacombe KR, Kreisl WC, Liow JS, Zoghbi SS, Telu S, Zhang Y, Pike VW, Halldin C, Gottesman MM, Innis RB, Hall MD. Lysosomal trapping of a radiolabeled substrate of P-glycoprotein as a mechanism for signal amplification in PET. *Proc. Natl. Acad. Sci. U.S.A*, **108**, 2593-2598 (2011).

III. **Kannan P**, Telu S, Shukla S, Ambudkar SV, Pike VW, Halldin C, Gottesman MM, Innis RB, Hall MD. The "specific" P-glycoprotein inhibitor tariquidar is also a substrate and an inhibitor for breast cancer resistance protein (BCRP/ABCG2). *ACS Chem. Neurosci.* **2**, 82-89 (2011).

LIST OF NON-THESIS PUBLICATIONS

I. **Kannan P**, John C, Zoghbi SS, Halldin C, Gottesman MM, Innis RB, Hall MD. Imaging the function of P-glycoprotein with radiotracers: pharmacokinetics and in vivo applications. *Clin. Pharmacol. Ther.* **86**, 368-77 (2009).

II. Kreisl WC, Fujita M, Fujimura Y, Kimura N, Jenko KJ, **Kannan P**, Hong J, Morse CL, Zoghbi SS, Gladding RL, Jacobson S, Oh U, Pike VW, Innis RB. Comparison of [^{11}C]-(*R*)-PK 11195 and [^{11}C]PBR28, two radioligands for translocator protein (18 kDa) in human and monkey: Implications for positron emission tomographic imaging of this inflammation biomarker. *Neuroimage* **49**, 2924-32 (2010).

III. Seneca N, Zoghbi SS, Shetty HU, Tuan E, **Kannan P**, Taku A, Innis RB, Pike VW. Effects of ketoconazole on the biodistribution and metabolism of [^{11}C]loperamide and [^{11}C]*N-desmethyl*-loperamide in wild-type and P-gp knockout mice. *Nucl. Med. Biol.* **37**, 335-45 (2010).

IV. Goldsborough A, Handley M, Dulcey A, Pluchino K, **Kannan P**, Brimacombe KR, Hall MD, Griffiths G, Gottesman MM. Collateral sensitivity of multidrug resistant cells to the orphan drug tiopronin. *J. Med. Chem.* **54**, 4987-97 (2011).

TABLE OF CONTENTS

LIST OF ABBREVIATIONS

ABC	ATP-binding cassette (transporter family)
ABCB1	Human gene that encodes for P-gp
abcb1a/b	Mouse genes that encode for P-gp
ABCC1	Human gene that encodes for MRP1
abcc1	Mouse gene that encodes for MRP1
ABCG2	Human gene that encodes for BCRP
abcg2	Mouse gene that encodes for BCRP
Aβ	Amyloid beta
ATP	Adenosine triphosphate
BBB	Blood-brain barrier
BCRP	Breast cancer resistance protein
$B_{\max}$	Receptor density
CsA	Cylcosporin A
dLop	*N-desmethyl*-loperamide
DMSO	Dimethyl sulfoxide
FTC	Fumitremorgin C
HPLC	High-performance liquid chromatography
i.v.	Intravenous
K_{D}	Dissociation constant at equilibrium
MRP1	Multiple resistance protein 1
PBS	Phosphate-buffered saline
PET	Positron emission tomography
P-gp	P-glycoprotein
SD	Standard deviation
SPECT	Single photon emission computerized tomography
SUV	Standard uptake value

1 INTRODUCTION

Efflux transporters are proteins that regulate the movement of molecules in and out of cells. These proteins, found in many different cell types of the body, can also prevent the entry of therapeutic drugs into cells and tissues. Drug efflux may therefore be a mechanism by which drug resistance occurs in disorders such as epilepsy or cancer. Understanding the function and density (or amount) of these transporters in the living body can improve or alter treatment options and can lead to the development of more targeted drugs. Radiolabeled molecules that interact with efflux transporters offer a powerful way to elucidate transporter function and density in healthy and diseased states.

1.1 ATP-BINDING CASSETTE TRANSPORTERS

To exert their effect on intracellular proteins, many drugs and molecules must pass through cell membranes by one of two forms of transport. The first form is passive transport, in which molecules pass through the membrane on their own or via a protein channel (carrier-mediated), without the use of energy. The second form is active transport, in which molecules are pumped through the membrane via a transporter protein that uses a chemical energy source, such as an electrochemical gradient or the molecule adenosine triphosphate (ATP). Energy-dependent transporters move molecules against a concentration gradient across cellular membranes [1].

A large number of active transporters are encoded by genes from the ATP-binding cassette (ABC) superfamily. The ABC genes seem evolutionarily important, as they are expressed in many prokaryotic and eukaryotic cells [2]. In the human genome, 48 genes encode for the ABC transporters and have been grouped into seven subfamilies (designated *ABCA-ABCG*) based on sequence homology. The ABC transporters are efflux pumps that are expressed in cellular membranes of various tissues and have varying substrate specificities [3, 4].

1.1.1 P-glycoprotein (P-gp)

Of the ABC transporter genes, *ABCB1* has been most studied because it encodes P-glycoprotein (P-gp, also called ABCB1 or MDR1), a 170-kDa protein widely expressed in plasma cell membranes of healthy human tissues and multidrug-resistant tumors [3, 5, 6]. The structural and functional characteristics of P-gp help explain its role under both physiological and pathophysiological conditions [4–7]. Structurally, the transporter consists of two interwoven transmembrane regions, each containing six transmembrane helices and an ATP-binding domain located intracellularly (Figure 1) [8–10]. The transmembrane helices of P-gp bind a broad range of compounds, known as substrates, with varying affinities to the transporter [3, 5, 11], while ATP hydrolysis initiates substrate efflux [7, 10]. The amino acid sequence of P-gp varies 80-97% among species, which can also account for species differences in substrate recognition [2, 12].

Functionally, P-gp regulates the transport of biologically important molecules, nutrients, hormones, and drugs into and/or out of cells [7, 13]. Although it transports substrates that tend to be hydrophobic, positively charged, or weak base molecules with a planar ring system [13], the transporter recognizes a wide range of compounds, including antiarrhythmics, antihistamines, cholesterol-lowering statins, and HIV protease inhibitors [3, 5].

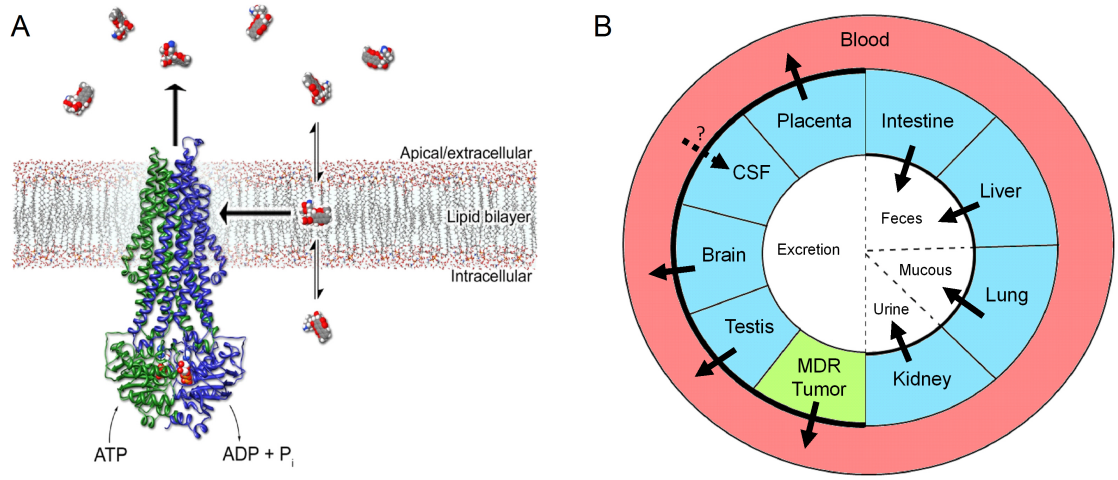

Figure 1. (A) Structural model of P-glycoprotein (P-gp) in the lipid bilayer showing extrusion of the P-gp substrate doxorubin (to scale). Binding and hydrolysis of ATP (shown bound during hydrolysis) initiates substrate extrusion. Substrates can be extruded directly from the lipid bilayer or be drawn from the intracellular pool. (B) P-gp pumps substrates out of organs of the human body in the direction indicated by the bold solid arrows. The thick black line indicates the barrier in which P-gp is located between various organs and the bloodstream; red indicates vasculature, blue represents tissue, and white indicates excreta. CSF, cerebrospinal fluid; MDR, multidrug resistance.

By regulating the intra- and extracellular concentration of molecules, P-gp helps maintain chemical homeostasis.

The transporter is widely expressed in the human body and plays both excretory and protective roles (Figure 1). Localization and pharmacokinetic studies have shown that P-gp can pump substrates out of tissue into the luminal space (blood), ultimately excreting substrates out of the body. To function in this excretory role, P-gp is widely expressed in cell membranes of organs such as the kidney, liver, and intestines [14–17]. In order to function in a protective role, P-gp is expressed in the membranes that create an interface between two organs. For example, at the blood-brain barrier (BBB) [18, 19], the blood-testes barrier [20, 21], and the placenta [22, 23], P-gp protects crucial organs (i.e., brain, testes, and fetus) against the entry of xenobiotics.

Although P-gp plays an important functional role, deletion or mutation of the gene encoding for P-gp is not lethal under laboratory conditions. For example, mice lacking the *abcb1a* and *abcb1b* genes (the mouse counterparts to the human *ABCB1* gene) are viable and healthy. The knockout mice do, however, tend to accumulate more toxins in their tissues than their wild-type counterparts [24]. In humans, some single-nucleotide polymorphisms and haplotypes (combinations of single-nucleotide polymorphisms) of the *ABCB1* gene have been shown to alter P-gp activity but do not impact function [25, 26]. In pathophysiological conditions, however, these mutations may be fatal. For example, patients with ovarian cancer who expressed the wild-type allele for P-gp had a mean progression-free survival of 19 months when treated with chemotherapy, whereas those expressing the G1199A polymorphism had a mean progression-free survival of only two months [27].

1.1.2 Breast cancer resistance protein (BCRP)

ABCG2 is an ABC gene that encodes for breast cancer resistance protein (BCRP), an 80-kDa protein known to confer multidrug resistance in cultured tumor cells [28–30]. Structurally, the transporter is unlike P-gp and MRP1 because it consists of only one ATP-binding domain and one drug-binding domain [31], and two BCRP transporters must combine as a homodimer to become functional [32, 33]. Functionally, BCRP is similar to P-gp: it recognizes a broad range of substrates (many of which are also P-gp substrates) [4, 31], and it is expressed in many of the same tissues as P-gp [16, 34–37]. For example, BCRP is expressed in the placenta to protect the fetus from exposure to toxic compounds that may circulate in maternal blood [36, 37]. The protein has additionally been found in tissues where P-gp is not expressed, such as in stem cells and mammary glands [38, 39]. Although BCRP's role is to protect organs and excrete compounds from the body, its role in pathophysiological conditions has not been explored extensively.

1.1.3 Multidrug resistance protein 1 (MRP1)

Another ABC transporter gene that is widely expressed in a range of tissues and in cancer cells is *ABCC1*, which encodes the 190-kDa multidrug resistance protein 1 (MRP1). The protein has one extra transmembrane domain than P-gp does [40] and tends to efflux substrates that are conjugates of organic anions (negatively-charged) or of glutathione [41]. Similar to P-gp, Mrp1 plays an excretory and protective role in the body and is frequently expressed in the same organs and barriers [42–45]. Because Mrp1 was discovered much later than P-gp, it has not been as well characterized and its involvement in pathophysiological conditions, other than in multidrug-resistant cancer, is unknown [11].

1.1.4 Definitions of terms: substrate, inhibitor, and competitive substrate

In the context of transporters, substrates are compounds that are transported, whereas inhibitors are compounds that restrict the function of the transporter [7, 46, 47]. The term inhibitor is often used synonymously with modulator, and the concepts are not clear-cut. For example, the compound verapamil is a substrate for P-gp at low concentrations, but, like many substrates, verapamil also inhibits ATP hydrolysis at high concentrations [48, 49]. Inhibitors, such as cyclosporin A and tariquidar, interfere with ATP hydrolysis at all concentrations [7, 46]. In this dissertation, the term *substrate* describes a drug transported by an ABC transporter, the term *inhibitor* describes a drug that restricts transporter function, and the term *competitive substrate* describes a drug that acts as both substrate and inhibitor, by saturating the transporter's capacity to efflux the substrate or by inhibiting ATP hydrolysis.

1.2 IMAGING P-GP AT THE BLOOD-BRAIN BARRIER

1.2.1 The blood-brain barrier (BBB)

Chemical homeostasis in the brain is maintained by the BBB, which limits the brain entry of toxins and substances circulating in the blood. The barrier is formed by the endothelial cells that line the walls of capillaries (small blood vessels) in the brain. In contrast to endothelial cells of capillaries in other tissues, those in the brain are joined to one another by tight junctions and do not contain fenestrations (Figure 2). Functionally, these properties serve

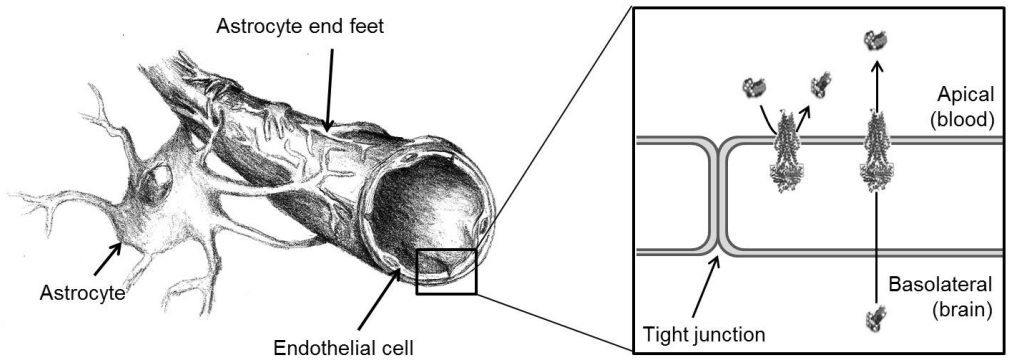

Figure 2. Diagram of the location of P-gp, BCRP, and MRP1 in the endothelial cells of brain capillaries. The walls of capillaries are lined with endothelial cells, which form tight junctions to prevent compounds from readily passing into the brain. The ABC transporters P-gp, BCRP, and MRP1 are located on the apical side of these polarized cells and facilitate the movement of compounds out of the brain or prevent the ingress of molecules into the brain.

to select the types of compounds that can readily cross the capillary walls into the brain. Small hydrophobic compounds, such as caffeine, can pass the barrier by passive diffusion, but large hydrophobic molecules and hydrophilic ones, such as hormones and amino acids, cannot. To mediate the entry of large molecules that are needed for brain function, the brain endothelial cells express a range of transporters. The glucose transporter isotype-1, for example, is highly expressed in these cells because glucose is the primary energy source for the brain [50].

The brain endothelial cells also express several transporters from the ABC family, with the most common ones – P-gp, BCRP, and several transporters of the *ABCC* family, including MRP1 – found on the apical (blood-facing) membrane of the cells (Figure 2) [18, 34, 42, 43]. While all three transporters are known to efflux drugs out of the brain, P-gp's role at the BBB has been extensively studied. P-gp immediately transports substrates that enter the apical membrane of the lipid bilayer of endothelial cells back into the blood and, therefore, prevents the penetration of toxic hydrophobic substances into neural tissue [3, 13]. The anti-diarrheal drug loperamide (Imodium®), for example, is an opiate that is sold over-the-counter because P-gp prevents it from crossing the BBB [13, 51]. Although P-gp prevents certain drugs from having side effects in the brain, it becomes an impediment to treating brain disorders if a drug cannot reach the intended target in the brain [52]. Thus, it is essential to measure the function and density of P-gp in both physiological and pathophysiological conditions.

1.2.2 Pathological conditions involving P-gp at the BBB

In vitro and animal data suggest that P-gp may play a role in disorders such as medication-refractory epilepsy and Alzheimer disease. Over-expression of P-gp is hypothesized to contribute to medication-refractory epilepsy, which is a condition in which a patient does not respond to several antiepileptic drugs. Biopsy specimens from patients with medication-refractory epilepsy showed a 130-200% increase in P-gp expression in cells immediately surrounding the epileptogenic focus (i.e. seizure-prone area). Seizures are known to not only transiently disrupt the BBB but also induce glutamate release, both of which signal nearby tissue to up-regulate P-gp expression [53, 54]. In contrast, under-expression of P-gp

may play a role in the development of Alzheimer disease, a form of dementia characterized in postmortem brains by senile plaques containing an insoluble form of amyloid beta (Aβ). Although the deposition of Aβ occurs in normal aging, the process is accelerated in Alzheimer disease [55, 56]. A postmortem study of brains from non-demented elderly patients showed that P-gp expression was significantly and inversely correlated to deposition of Aβ suggesting that P-gp might play a role in controlling Aβ deposition in the brain [57]. In vitro experiments showed that Aβ is a substrate for P-gp, and imaging studies with radioactive Aβ_{40} injected intracranially in wild-type and P-gp knockout mice showed that knockout mice had greater Aβ deposition than wild-type mice [55]. Because in vitro samples do not always represent the in vivo situation, these studies highlight the importance of measuring P-gp function and expression in the living BBB.

1.2.3 Imaging using positron emission tomography

Positron emission tomography (PET) and single photon emission computerized tomography (SPECT) are nuclear imaging techniques regularly used to visualize and measure in vivo processes with great sensitivity. For imaging in vivo, a molecule is tagged with a radioactive isotope and injected at tracer (subpharmacological) doses into the body. The decay characteristics of the radioisotope are then measured and reconstructed into an image that shows the spatial distribution of the molecule. In PET, radioisotopes, such as ^{11}C or ^{18}F, are unstable atoms that contain fewer neutrons than the stable isotope (^{12}C or ^{19}F) and therefore decay (or release energy) by positron emission to become stable (Figure 3). In the decay process, a proton is converted into a neutron and a neutrino and positron are released. The positron, the antimatter counterpart of an electron, travels a short distance until it collides with an electron and annihilates. During annihilation, the masses of the two particles are converted into energy in the form of two identical gamma rays, which are then detected by a PET camera and used to reconstruct a three-dimensional image [58].

PET typically quantifies the pharmacokinetics of a radiolabeled drug that binds with high affinity to a specific receptor target. Through modeling, pharmacokinetic parameters are then used to determine the so-called binding potential of the receptor site; the binding potential is the product of receptor density and the affinity of the radioligand for the receptor [59]. In the case of the efflux transporter P-gp, PET can quantify not only density but also function. Inhibitors known to bind to P-gp with high affinity have been radiolabeled and evaluated for their ability to measure P-gp density in the brain [60–63]. On the other hand, substrates of P-gp have been used to measure P-gp function, where function is implied by the absence of substrate in a P-gp protected organ rather than its presence. P-gp function can then be quantified using PET by measuring the difference in uptake of a radiolabeled substrate in the target tissue before and after inhibition of the transporter [64–67]. Under baseline conditions, the protected organ or tumor accumulates minimal amounts of the radiolabeled substrate, and after P-gp inhibition, the organ accumulates far more substrate. In a tissue in which P-gp is absent or dysfunctional, the uptake of substrate should be unaffected by inhibition [68].

1.2.4 Selection criteria for radiotracers that image P-gp

Although imaging of P-gp function and density is a relatively new area of research, several criteria are important for the selection of an optimal radiolabeled tracer: radiochemical purity of the signal, selectivity for P-gp, and magnitude of the signal.

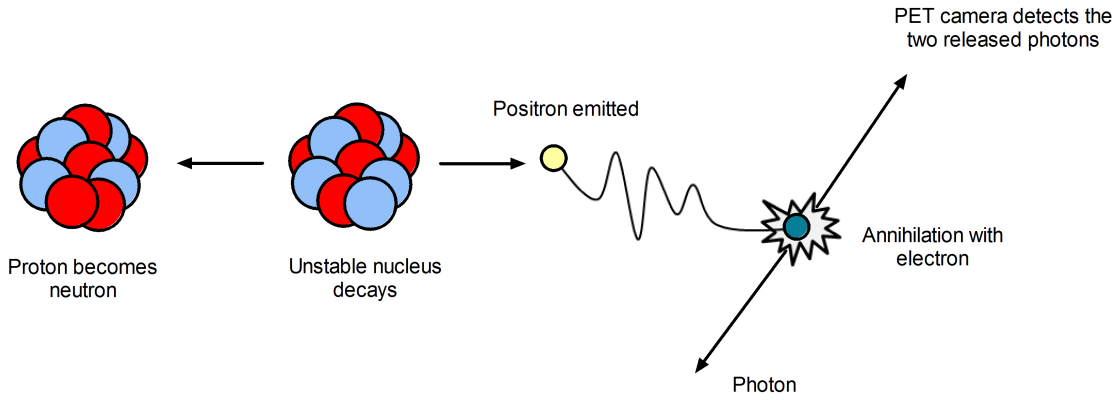

Figure 3. Representation of the decay process of a positron-emitting radionuclide. The radioactive atom contains an unstable nucleus, which decays to become stable; a proton is converted to a neutron and a positron is emitted to balance out the charge. The positron, the antimatter counterpart of an electron, travels a short distance until it annihilates with an electron. In the process, two identical photons are released 180 degrees apart from one another and are detected by the PET camera.

To ensure accurate quantification, the signal measured from the radiotracer must be radiochemically pure because SPECT and PET measure total radioactivity and cannot distinguish radioligands from radiometabolites. For example, if a radiometabolite that is not a substrate for P-gp enters the target tissue, it will increase the baseline signal and thereby blunt the relative magnitude of the signal after P-gp inhibition [69]. The presence of radiometabolites can be measured in animal models (e.g., P-gp knockout and wild-type mice), but the generation of radiometabolites in animals does not always reflect the situation in humans [70, 71]. When metabolism of a radiotracer occurs, the tracer can sometimes be redesigned to avoid a particular metabolic route, as it is desirable to use a radioligand that has little to no metabolism [69].

A second criterion for an optimal radiotracer for P-gp is its selectivity for the transporter. Selectivity is critical because of the varying expression of a number of transporters in the body and the common occurrence of cross-recognition of substrates and inhibitors [4]. A range of in vitro assays can be used to identify if a candidate substrate radiotracer is selective for P-gp. One such method is the Transwell-transport assay that uses polarized cell lines, such as Madin-Darby canine kidney and colorectal adenocarcinoma (Caco-2) cells, that are engineered to overexpress a range of human ABC transporters. These cells are grown as an epithelial layer on Transwell inserts and form tight junctions that prevent paracellular diffusion of compounds; a given molecule can therefore traverse the well by passive diffusion or transporter-mediated processes. A compound is identified as a substrate for P-gp, for example, if it is transported from the basolateral to the apical side, and if transport in the reverse direction is prevented. Furthermore, the transport from the basolateral to apical side should be blocked by P-gp inhibitors [72, 73]. The selectivity of a compound for P-gp can thereby be assessed, using cells expressing various ABC transporters. Another method is to measure a substrate's intracellular accumulation in cell lines expressing various ABC transporters; a compound is identified as a substrate for P-gp if the control cells accumulate more substrate than the P-gp-expressing cells. This accumulation assay is arguably easier to perform than that with polarized cells and has been proven to be a good indicator of transport selectivity. For both assays, selectivity can also be confirmed

by using inhibitors to block transport or accumulation of substrate [68]. Other biophysical assays are available to further probe drug-transporter interactions; these include ATPase assays in vesicles, substrate competition assays, and time-course kinetics of transport [7]. Candidate radiolabeled substrates selected from in vitro assays can be then be tested in vivo in knockout mice to confirm selectivity. For example, a candidate substrate that is selective for P-gp should have enhanced uptake in the brains of mice that lack P-gp [68].

Selectivity of a candidate inhibitor radioligand for P-gp can also be measured in vitro. One method is to add the putative P-gp inhibitor along with a fluorescent substrate to ABC transporter-expressing cells. The cellular uptake of the substrate is then measured; if fluorescence uptake increases, then the inhibitor interacts with that transporter [74, 75]. The cellular accumulation assay also measures inhibitor selectivity, where a radiolabeled inhibitor is added to both control and ABC transporter-expressing cells. Higher "accumulation" is expected in the transporter-expressing cells than in control cells if the inhibitor binds to the transporter [76]. The selectivity of that compound can thereby be assessed using cells expressing various ABC transporters. Finally, ATPase assays can be used to verify that the inhibitor does not stimulate ATPase activity, which is essential for ABC transporter function [7].

A third criterion for an optimal radiolabeled tracer for P-gp is the magnitude of the signal, which is measured differently for a substrate and an inhibitor. For a substrate, the magnitude of signal is the ratio of the amount of compound in the tissue at baseline to the amount after P-gp blockade. Because in vivo imaging has limited anatomic resolution, the visual effects in small organs become blurred or spill into their surroundings, an effect called the "partial volume error" [58]. Furthermore, variations between species and tissues in the expression of P-gp should be taken into account when assessing the suitability of the radiotracer [12]. The magnitude of the signal measured in most in vitro assays of a substrate is therefore diminished when measured in vivo. For an inhibitor, the magnitude of signal is the binding potential, which is the product of the density of receptors ($B_{\max}$) and the affinity ($1/K_{\mathrm{D}}$ of the inhibitor for the target). In vivo, binding potential can be expressed as the ratio of specific binding to non-specific binding [59].

1.2.5 Radiolabeled substrates for imaging P-gp function

Many substrates of P-gp, such as sestamibi, verapamil, daunorubicin, colchicine, and *N-desmethyl*-loperamide (dLop), have been radiolabeled for SPECT and PET imaging of P-gp function at the BBB [64, 68, 77–80]. Although all of these were evaluated in animals, only three were extended to assessment in humans: [^{99m}Tc]sestamibi, [^{11}C]verapamil, [^{11}C]dLop.

Sestamibi The SPECT agent [^{99m}Tc]methoxyisobutylisonitrile ([^{99m}Tc]sestamibi) is a positively charged lipophilic complex (Figure 4) that readily enters cells in the absence of P-gp. The radiotracer was found to measure P-gp function in cell lines and in various drug-resistant tumors in vivo [68, 81], but it is not the most ideal substrate radiotracer. Although [^{99m}Tc]sestamibi is known to produce a radiochemically pure signal [82], it is a substrate for both P-gp and MRP1, decreasing its utility to image the function of only P-gp. Furthermore, the magnitude of signal produced by [^{99m}Tc]sestamibi is smaller than those produced by other substrate radiotracers. For example, brain uptake of [^{99m}Tc]sestamibi by ex vivo measurements in P-gp knockout mice was only four-fold higher than in wild-

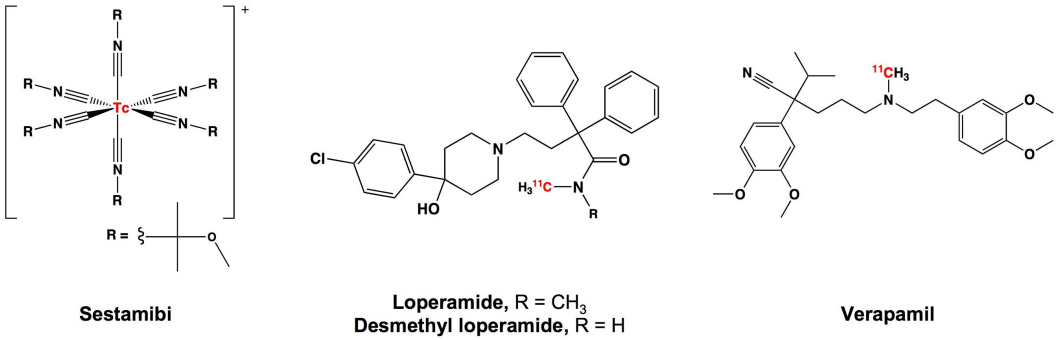

Figure 4. Chemical structures of P-gp substrates radiolabeled for SPECT and PET imaging. The radiolabeled atom is indicated in red.

type mice [68]. Thus, of the three criteria for a substrate radiotracer described earlier, [^{99m}Tc]sestamibi fulfills one (radiochemical purity) and marginally fulfills a second (magnitude of signal).

Verapamil [^{11}C]Verapamil (Figure 4) is a calcium channel blocker and is both a substrate and inhibitor of P-gp [77]. At the low concentrations used in PET, [^{11}C]verapamil functions as only a substrate and therefore has been extensively used to measure P-gp function [7, 78, 83]. However, it also does not fulfill the three criteria for a substrate radiotracer. For one, [^{11}C]verapamil undergoes extensive oxidative metabolism by cytochrome P450 enzymes in humans, and some of the radiometabolites of [^{11}C]verapamil have substrate activity at P-gp [84, 85]. Furthemore, [^{11}C]verapamil is not selective for P-gp as it has been reported to modulate the activity of MRP1 [86]. The radiotracer does, however, fulfill the third criterion because it produces a large magnitude signal in the absence of P-gp, as the brain uptake of [^{11}C]verapamil in P-gp knockout mice was ten-fold higher by ex vivo measurements than that in wild-type mice [77, 78]. Nevertheless, the radiometabolites of [^{11}C]verapamil and its interaction with MRP1 significantly limit the radiotracer's ability to quantify P-gp function.

dLop Loperamide is a potent over-the-counter opiate used to treat diarrhea, but it lacks effects in the central nervous system because it is an avid substrate for P-gp at the BBB [51]. A major metabolite of loperamide in animals and humans is dLop, which also behaves as a substrate for P-gp. Injection of the metabolite, [^{11}C]dLop, rather than the parent compound, [^{11}C]loperamide, markedly decreases the concentration of further radiometabolites that enter the brain [69] because dLop is metabolically stable.

[^{11}C]dLop (Figure 4) shows promise as a substrate radiotracer of P-gp. The radiotracer has high signal purity because it produces minimal ($\leq$ 10%) radiometabolites that enter brains of P-gp knockout mice, measured ex vivo at 30 minutes [64]. With regard to selectivity, uptake of the radiotracer was markedly enhanced in the brains of P-gp knock-

out mice and of monkeys after blockade by inhibitors selective for P-gp [64, 67]. However, these studies do not definitively prove selectivity for P-gp because dLop's interaction with the other two major transporters at the BBB (BCRP and MRP1) is unknown, and systematic in vitro assays with various ABC transporters would be more conclusive. Finally, [^{11}C]dLop also demonstrates high signal strength because brain uptake of [^{11}C]dLop by ex vivo measurements was seventeen-fold higher in P-gp knockout mice than in wild-type mice [64]. Although the magnitude of this signal is blunted in PET imaging by the limited anatomic resolution of PET, [^{11}C]dLop is trapped in the brain upon entry, despite declining plasma concentrations [87, 88]. From an imaging perspective, this irreversible trapping is beneficial because it amplifies the PET signal by accumulating radioactivity over time. Although dLop is an opiate agonist, its trapping is not a result of high-affinity binding to the opiate receptor [64], i.e. the mechanism of trapping is unknown.

1.2.6 Radiolabeled inhibitors for imaging P-gp density

Substrate radiotracers such as [^{11}C]dLop cannot be used directly to measure the expression, or density, of P-gp at the BBB, because they do not bind to the transporter in a classical receptor-ligand fashion [59, 68]. Instead, inhibitors such as elacridar and tariquidar that are known to bind to P-gp with high affinity have been radiolabeled and evaluated for their ability to measure P-gp density in the brain [60–63].

Elacridar The synthetic compound elacridar (Figure 5) has been extensively studied because of its high affinity for P-gp (K_D = 0.8 nM) [89] and its high potency to inhibit P-gp at nanomolar concentrations ($\geq$ 20 nM) [90]. Because of its high binding affinity to P-gp, elacridar was radiolabeled and injected in animals with the aim of mapping out the distribution of P-gp in the brain [61, 63, 91]. However, elacridar does not fulfill two of the three criteria of an ideal radioligand: although [^{11}C]elacridar has good metabolic stability in vivo and high specific binding in vitro, elacridar also inhibits BCRP function [92], thus lacking selectivity. In addition, the radiotracer has a low magnitude of signal in wild-type mouse brain [61, 63, 91]. Therefore, the lack of selectivity and the low magnitude of signal limit the usefulness of this radiotracer.

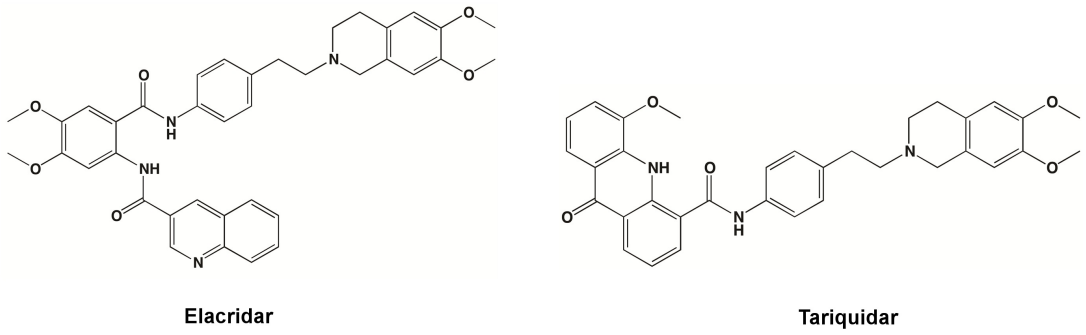

Figure 5. Chemical structures of two high-affinity inhibitors of P-gp that have been radiolabeled for PET imaging.

Tariquidar Tariquidar (Figure 5) has been routinely used to inhibit P-gp function in vitro and in vivo because of its high affinity for P-gp (K_D = 5 nM) [46], its ability to inhibit P-gp at nanomolar concentrations ($\geq$ 40 nM) [93], and its relatively low toxicity [94]. Tariquidar was radiolabeled and injected in animals in order to map out the distribution of P-gp in the brain [60, 62], but the results of the imaging studies indicate that [^{11}C]tariquidar may not fulfill two of the three criteria of an ideal radioligand. [^{11}C]Tariquidar is metabolically stable, as 96% of the radioactivity in plasma measured 20 min after injection is the parent [62]. However, its selectivity for P-gp is uncertain, as micromolar concentrations of the compound has been reported to inhibit the function of BCRP [75]. Furthermore, the radiotracer has a low magnitude of signal because its uptake in brain is very low [60, 62], but the reason for this low uptake is unclear.

2 AIMS

The aims of this thesis were to determine the pharmacological properties of radiotracers used to image P-gp function and density. Both cell culture techniques and PET imaging were used when possible to ensure that the property of the radiotracer found in vitro paralleled that found in vivo.

1. To characterize the selectivity of [^{11}C]dLop as a substrate for P-gp (paper I)
2. To understand the mechanism of dLop's trapping in the brain (paper II)
3. To characterize the selectivity of [^{11}C]tariquidar as an inhibitor for P-gp (paper III)
4. To investigate whether tariquidar can measure P-gp density in vitro

3 MATERIALS AND METHODS

The pharmacological properties of the P-gp substrate dLop and the P-gp inhibitor tariquidar were evaluated both in vitro and in vivo. A summary of the materials and methods used in the studies is described in this chapter, with more detailed information provided in the full papers located in the second half of the book.

3.1 CHEMICALS

3.1.1 Radiotracers

For cell and post-mortem studies, dLop and tariquidar were radiolabeled. For cell studies, [*N-desmethy*l-^{3}H]dLop (American Radiolabeled Chemicals) was synthesized as described previously [64] and [*O-methyl*-^{3}H]tariquidar (American Radiolabeled Chemicals) was synthesized by [$^{3}H_3$]methylation of *O-desmethyl*-tariquidar. Both compounds had a radiochemical purity > 97.7% by HPLC analysis, a specific activity of 3.0 GBq/μmol, and a concentration of 37 MBq/mL. For post-mortem brain studies, [*O-methyl*-^{3}H]tariquidar had a radiochemical purity > 98% by HPLC analysis, a specific activity of 1.7 GBq/μmol, and a concentration of 4.4 MBq/mL.

For small animal PET studies, the radiotracer [^{11}C]dLop was prepared [64] and obtained in high radiochemical purity (99%) and with a specific activity of 90.0 $\pm$ 34.9 GBq/μmol (n = 5 batches) at the time of injection. For human PET studies, [^{11}C]dLop was prepared [64], in accordance with an investigational new drug application (101,092) submitted to the US Food and Drug Administration (http://pdsp.med.unc.edu/snidd/). The radiotracer was obtained in high radiochemical purity (100%) and with a specific activity of 116 $\pm$ 46 GBq/μmol (n = 12 batches) at the time of injection.

3.1.2 Pharmacological agents

For cell and post-mortem brain studies, all pharmacological agents were dissolved in DMSO or ethanol before dilution in culture media or saline buffer. For mouse PET studies, tariquidar solution (7.5 mg free base/mL; gift from Susan Bates, National Cancer Institute, Bethesda, MD, USA) was diluted 1:10 in 0.9% saline. For human PET studies, tariquidar solution was supplied by AzaTrius Pharmaceuticals and prepared as before [88].

3.2 IN VITRO STUDIES

3.2.1 Cell lines

Four pairs of cell lines were cultured, each pair consisting of a parental (control) and a resistant (ABC transporter-expressing) line. Resistant cell lines were sub-cultured from parental cells, and expression of ABC transporters was maintained by addition of cytotoxic drugs to culture media (Table 1) [95–98]. The KB, MCF7, and NIH cell lines were cultured in Dulbecco's modified Eagle's medium, whereas the H460 cell lines were cultured in Roswell Park Memorial Institute 1640 medium. Culture media were supplemented as reported [99] and cell lines were grown at 37 °C in 5% CO_2 [95].

Table 1. Expression of ABC transporters in four pairs of cell lines derived from human and mouse tissues.

Tissue source	Cell type	Cell line name	ABC transporter	Drug used for expression
Human adenocarcinoma	B1 parental	KB-3-1	–	–
	B1 resistant	KB-8-5-11	P-gp	Colchicine (250 nM)
Human large-cell lung cancer	G2 parental	H460	–	–
	G2 resistant	H460/MX20	BCRP	Mitoxantrone (20 nM)
Human breast cancer	C1 parental	MCF-7	–	–
	C1 resistant	MCF-7/VP16	MRP1	Etoposide (4 μM)
Mouse fibroblasts	*b1* parental	NIH-3T3	–	–
	b1 resistant	NIH-C3M	P-gp	Colchicine (2.5 μM)

3.2.2 Brain tissues

Brain sections were prepared and cut for labeling of P-gp. Four strains of mice (Taconic Farms, Germantown, NY) were used: wild-type (model FVB), P-gp knockout (*abcb1a/b*$^{-/-}$; model 001487), BCRP knockout (*abcg2*$^{-/-}$; model 002767), and P-gp/BCRP dual knockout (*abcb1a/b*$^{-/-}$*/abcg2*$^{-/-}$; model 003998). Mouse brains were rapidly removed after decapitation, snap frozen in liquid nitrogen, and stored at -70 °C.

All brains were thawed to -20 °C, cut in coronal or sagittal slices of 10 μm thickness at -20 °C using a cryostat (Jung-Frigocut 2800E, Leica, Heidelberg, Germany), dried on Superfrost-treated glass slides and stored at -25 °C until the day of the experiment [100]. Mouse experiments were approved by the ethical committee at Karolinska Institutet.

3.2.3 Radioaccumulation studies

For selectivity and ionic trapping studies, accumulation of low concentrations of radiotracers was measured in human cell lines using the following protocol. Cells were seeded at a density of 2.5 x 10^5 cells/well in 24-well plates and incubated in culture media for 24 h at 37 °C to allow attachment. The time course of accumulation for each radiotracer was measured in KB-3-1 cells to determine when the radiotracer accumulation stabilized (i.e. did not continue to increase). All subsequent experiments were conducted for 45 min for [^{3}H]dLop and for 240 min for [^{3}H]tariquidar in different cell lines. If necessary, cells were pre-treated for 30 min at 37 °C with increasing concentrations of a pharmacological agent before they were incubated with [^{3}H]dLop (1 nM) or [^{3}H]tariquidar (1 nM) at 37 °C unless specified. After incubation, cells were washed with ice-cold phosphate buffered saline (PBS, 1X) and lysed with trypsin for 90 min at 37 °C. Radioactivity in the lysates was measured with liquid scintillation counting.

For studies on the ionic trapping of dLop, two different experimental conditions were used. In the first condition, control (KB-3-1) cells were pretreated with bafilomycin A and tamoxifen to test whether dLop (pK_a of 7.3; [64]) is trapped as protonated weak base in acidic lysosomes (Figure 6). Bafilomycin A is a compound that prevents the acidification of

the lysosome by inhibiting the proton vacuolar-ATPase [101] whereas tamoxifen is a weak base (pK_a of 8.5) that accumulates within lysosomes and depletes the free proton pool [102]. We also used unlabeled dLop itself to compete for cellular accumulation. In the second condition, accumulation was measured in control (KB-3-1) and P-gp-expressing (KB-8-5-11) cells pretreated with increasing concentrations of tariquidar because the in vivo trapping of [^{11}C]dLop in brain tissue occurs in the presence of the inhibitor tariquidar [88].

For studies on the ionic trapping of tariquidar, [^{3}H]tariquidar accumulation was measured in control (KB-3-1) cells pretreated with tamoxifen and chloroquine, another weak base (pK_as 8.5 and 10.8) [103].

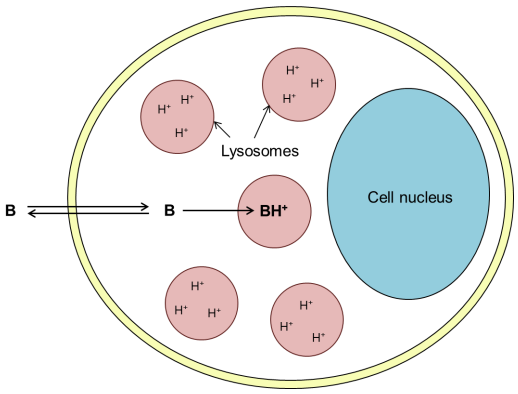

Figure 6. Schematic model demonstrating how a weak base, **B** passively diffuses into a cell and then becomes irreversibly trapped by protonation (**BH**$^{+}$) in acidic lysosomes (red). When lysosomal pH increases (i.e. becomes more basic), the lysosomal accumulation of the weak base decreases.

3.2.4 Inhibition of transporter function

The selectivity of dLop and tariquidar as an inhibitor for each ABC transporter was measured by the uptake of a fluorescent substrate (one preferentially effluxed by P-gp, BCRP, or MRP1) in the presence of increasing concentrations of dLop or tariquidar. Three conditions for each transporter were measured: untreated (negative control), inhibitor-treated (positive control), and dLop/tariquidar-treated. Cells (2 x 10^5) were suspended in 1 mL of Iscove's modified Dulbecco's medium containing 5% fetal bovine serum and were pretreated for 10 min at 37 °C with media containing either an inhibitor or dLop/tariquidar. Following pretreatment, cells were resuspended in media containing the same inhibitor used during pretreatment and a fluorescent substrate. The following fluorescent substrates were used: 4 μM rhodamine 123 for P-gp, 5 μM mitoxantrone for BCRP, and 0.25 μM calcein-AM for MRP1 [26, 74]. Although calcein-AM is not itself a substrate of MRP1, it is cleaved by cellular esterases to yield fluorescent calcein, which is effluxed by MRP1 [104]. Following incubation in the dark for 45 min at 37 °C, cells were centrifuged and resuspended in 300 μL of PBS containing 0.1% bovine serum albumin. Fluorescence intensity was recorded for a total of 10,000 cells using a FACSCalibur flow cytometer (BD Biosciences, San Jose, CA, USA).

3.2.5 Confocal microscopy

To visually confirm that dLop and tariquidar are trapped in lysosomes, we examined their ability to displace a fluorescent weak base from lysosomes using confocal microscopy. Cells (2.5 x 10^5/well) were seeded onto glass coverslips in 6-well plates and allowed to attach over 24 h at 37 °C. They were then incubated for 30 min at 37 °C with three compounds simultaneously: 10 nM Lysotracker (a fluorescent lysosomal marker that is a weak base), 8 μM Hoechst 33342 (a fluorescent nuclei marker), and either DMSO, dLop, tamoxifen (positive control), or paclitaxel (negative control). After treatment, coverslips were

removed from media, washed in PBS, inverted onto glass slides, and sealed. Cells were imaged using a Zeiss LSM 510 UV microscope (Carl Zeiss Microimaging, Germany).

3.2.6 ATPase assay

The beryllium fluoride-sensitive ATPase assay was used to investigate whether tariquidar stimulates the ATPase activity of BCRP as previously described [105]. In brief, membrane vesicles (10 μg of protein) of High Five insect cells were incubated with varying concentrations of tariquidar in the presence and absence of beryllium fluoride (BeFx; 0.2 mM beryllium sulfate and 2.5 mM NaF) in ATPase assay buffer for 5 min. The reaction was started by the addition of 5 mM ATP and was stopped by the addition of 0.1 mL of 5% sodium dodecyl sulfate solution after 20 min. The amount of inorganic phosphate released and the BeFx-sensitive ATPase activity of ABCG2 was determined as described previously [105].

3.2.7 Autoradiography

P-gp density in mouse brain was measured as the binding of [^{3}H]tariquidar in brains of wild-type and P-gp knockout mice. Sagittal slices (10 μm) of each brain from 3 mice per strain were preincubated for 30 min at 22 °C with increasing concentrations of tariquidar and cyclosporin A (Sigma Aldrich, St. Louis, MO, USA) made in PBS containing 0.3% bovine serum albumin (Sigma Aldrich, St. Louis, MO, USA). Slices were then incubated in the same solution now containing 1 nM [^{3}H]tariquidar. The time course of binding was measured in wild-type mouse brain at 4 and 22 °C to determine when tariquidar binding reached equilibrium. Subsequent experiments in mouse brains were conducted for 120 min at 22 °C. After incubation, brain slices were washed 3 x 10 min in ice-cold PBS (1X), dipped in distilled water and allowed to dry. Radioactivity was measured after slides were exposed to phosphor imaging plates (BAS IP-TR 2040, Fuji Photo Film Co., Japan) for four days and scanned using a Fujifilm BAS-5000 scanner (Tokyo, Japan).

3.3 IN VIVO STUDIES

3.3.1 Imaging in animals

Imaging studies of dLop selectivity were performed in wild-type, P-gp knockout (*abcb1a/b*$^{-/-}$), BCRP knockout (*abcg2*$^{-/-}$), and MRP1 knockout (*abcc1a*$^{-/-}$) mice, while studies of lysosomal trapping were performed in P-gp knockout mice (Taconic Farms, Germantown, NY, USA). Animal experiments were performed in accordance with the *Guide for Care and Use of Laboratory Animals* [106] and were approved by the National Institute of Mental Health Animal Care and Use Committee.

All PET studies performed in mice were conducted using the following protocol. In brief, animals were anesthetized using 1.5% isoflurane through a nose cone, injected via the tail vein with [^{11}C]dLop or a pharmacological agent, and scanned using a Focus 220 microPET camera (Seimens Medical Solutions, Knoxville, TN, USA). To study the in vivo selectivity of dLop for ABC transporters, four strains of mice were injected with [^{11}C]dLop (16.0 $\pm$ 4.6 MBq; 0.1 mL) and radioactivity uptake was measured in their brains. To study the lysosomal competition between dLop and tariquidar in vivo, P-gp knockout mice were first treated with 100 μL saline and tariquidar (32 mg/kg). After 30 min, [^{11}C]dLop (7.8 $\pm$ 1.3 MBq; 0.1 mL) was injected and radioactivity uptake was measured in kidneys and

spleen, which are lysosomal-rich organs. Mice from different strains or different treatments were imaged simultaneously because the Focus 220 can accommodate up to 6 mice in a single scan. Body temperatures were maintained between 36.5 °C and 37 °C using a heating pad or lamp. Serial dynamic scans were collected for 60 min and were reconstructed using a Fourier rebinning + 2D ordered-subset expectation maximization algorithm, resulting in an image resolution of 1.6 mm at full-width at half maximum. No attenuation or scatter-correction was applied.

3.3.2 Imaging in human subjects

Six healthy volunteers (age 33 $\pm$ 10 y) were selected based on previously published criteria. In brief, subjects were free of current medical and psychiatric illness based on screening tests and were also free of any medication for at least 3 d before and after administration of tariquidar. Human studies were performed in accordance to our Investigational New Drug Application submitted to the Food and Drug Administration and were approved by the local Institutional Review Board.

To study the lysosomal competition between dLop and tariquidar in vivo, volunteers underwent whole-body PET scans of [^{11}C]dLop at baseline and after administration of tariquidar (2 mg/kg or maximal dose of 150 mg i.v.). Subjects had the second PET scan (after tariquidar administration) performed under identical conditions on the same day (n = 2 subjects) or on a following day (n = 4 subjects). For each subject, tariquidar was infused via the antecubital vein at a rate of 375 mL/h just before injection of [^{11}C]dLop. The injected dose of [^{11}C]dLop was 663 $\pm$ 83 MBq at baseline and 639 $\pm$ 93 MBq after administration of tariquidar. Images were then acquired on a high resolution research tomograph PET camera from 5 to 120 min as before [88]. Attenuation correction was applied as previously reported [88].

Subjects were monitored for blood pressure, temperature, heart rate, and respiration rate before and after administration of tariquidar, and after injection of [^{11}C]dLop. Blood and urine laboratory tests were repeated within 24 h after completion of the study.

3.4 DATA AND STATISTICAL ANALYSIS

3.4.1 In vitro studies

For radioaccumulation assays, the amount of radioactivity measured in lysates was first corrected for adsorption of the radiotracer to the plate and for cell count, and then standardized to radioactivity measured in control cells. Concentration-response curves were fitted and analyzed by nonlinear regression by using a log-sigmoidal model with variable slope (Prism 5.0, GraphPad software). After data were tested for homogeneity of variance, statistical significance was evaluated by the Student *t* test (unpaired, two-tailed, α = 0.05). Data are expressed as mean $\pm$ SD (n = 3-6 observations).

For studies on inhibition of transporter function, fluorescence data were analyzed using FlowJo software (Tree Star, Inc., Ashland, OR, USA) and mean values of fluorescence were averaged and standardized to the control cells. Data represent mean $\pm$ SD (n = 3-6 observations).

For the BCRP ATPase assay, the basal activity was subtracted to calculate percent stimulation in the presence of tariquidar. Data are expressed as mean $\pm$ SD (n = 3 observations).

For autoradiography studies, images were analyzed using Multi Gauge 3.2 (Fuji Photo Film Co., Japan). Regions of interest were drawn around each brain, and radioactivity was measured as the intensity of photon emissions (from the radiotracer) per unit area and corrected for background. Data were then analyzed using Prism 5.0 and are expressed as mean $\pm$ SD (n = 3 observations).

3.4.2 In vivo studies

For PET studies, reconstructed images were used to measure the concentration of radioactivity (decay-corrected till injection time) in each organ. Images were analyzed using Pixelwise Modeling Computer Software (PMOD Group, Zurich, Switzerland). Regions of interest (an outline defining the boundaries of an area) were drawn on coronal slices of the target organ for both mice and humans. The concentration of radioactivity (decay-corrected until injection time) was expressed as the standardized uptake value (SUV), which normalizes for injected activity and body weight.

$$SUV = \frac{activity\ per\ g\ of\ tissue}{total\ injected\ activity} \times body\ weight \tag{1}$$

Time-activity curves were created for each organ by plotting SUV versus time or %SUV versus time, and the area under the time-activity curve (i.e. SUV $\cdot$ min) of each organ was calculated by using the trapezoidal method of integration.

For mouse imaging studies, differences in mean area-under-the-curve (SUV $\cdot$ min) were compared by using one-way analysis of variance followed by the Bonferroni posttest for multiple comparisons (α = 0.05). Data are expressed as mean $\pm$ SD (n = 3-4 animals).

For human imaging studies, differences in the area under the time-activity curve (SUV $\cdot$ min) of each organ were compared between the baseline and tariquidar-treated condition by paired *t* test, and correction for multiple corrections was performed using the false discovery rate with a threshold of 0.05. Data are represented as mean $\pm$ SD (n = 5-6 subjects).

4 RESULTS AND DISCUSSION

4.1 PROPERTIES OF *N-DESMETHYL*-LOPERAMIDE (dLop)

4.1.1 dLop is a selective substrate for P-gp (paper I)

The selectivity of dLop at low concentrations (nanomolar) for P-gp, BCRP, and MRP1 was measured as its uptake in human and mouse tissues (Figure 7). In human cell lines, control (non-P-gp-expressing) cells of the ABCB1 pair accumulated 4 times more [^{3}H]dLop than P-gp-expressing cells ($P < 0.001$). In contrast to the findings in the ABCB1 pair, [^{3}H]dLop accumulation was not different between the control and transporter-expressing cells of the ABCG2 ($P = 0.18$) and ABCC1 ($P = 0.86$) pairs. In mice, similar results were obtained: the brain concentration of [^{11}C]dLop in P-gp knockout mice was at least 2.5-fold higher than that in MRP1 knockout, BCRP knockout, or wild-type mice ($P < 0.0001$). Taken together, these results are consistent with dLop behaving as a selective substrate for P-gp.

Because high concentrations of substrates can inhibit ABC transporter function, the selectivity of dLop at high concentrations (micromolar) for P-gp, BCRP, and MRP1 was also measured by its ability to inhibit the efflux of another fluorescent substrate. In human cells, we found that the uptake of a fluorescent P-gp substrate was at least 4-fold higher in P-gp-expressing cells treated with $\geq$ 20 μM dLop than in untreated ones (Figure 8). dLop did not inhibit BCRP or MRP1 function at any tested concentrations. As a positive control, inhibitors specific for each ABC transporter demonstrated inhibition of efflux in each transporter-expressing cell line. Although BCRP-expressing cells treated with fumitremorgin C had higher uptake of BCRP substrate than control cells did, this result was not anomalous because the control cells of the ABCG2 pair are known to express a small amount of functional BCRP [97]. Thus, dLop selectively inhibits P-gp function as a competitive substrate, a behavior consistent with that of other P-gp substrates, such as verapamil [7].

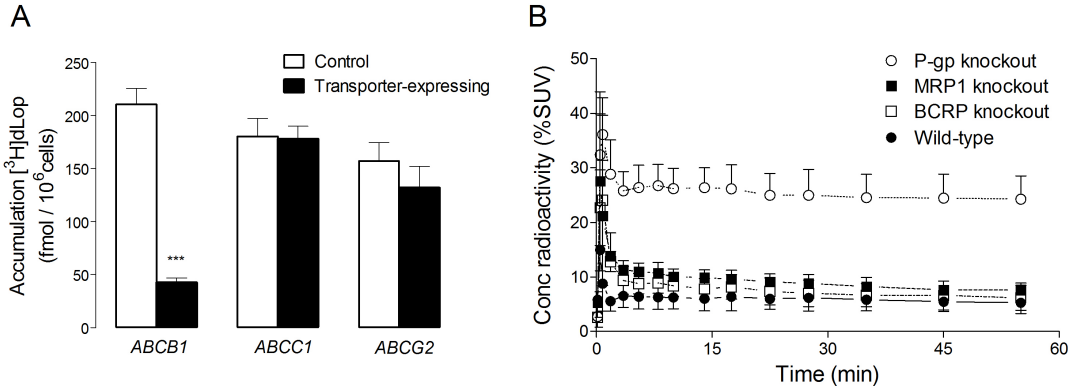

Figure 7. The selectivity of dLop as a substrate for three ABC transporters measured in human cell lines and transgenic mice. (A) [^{3}H]dLop accumulation is significantly different ($P < 0.001$) between the control and transporter-expressing cells of only the *ABCB1* pair. Bars represent mean $\pm$ SD (n = 3). (B) Concentration of radioactivity (%SUV) measured by PET after injection of [^{11}C]dLop is 2.5 times higher in P-gp knockout mice (○) than that in the other three strains of mice (BCRP knockout (■), MRP1 knockout (□), wild-type (●). Symbols represent mean $\pm$ SD (n = 3).

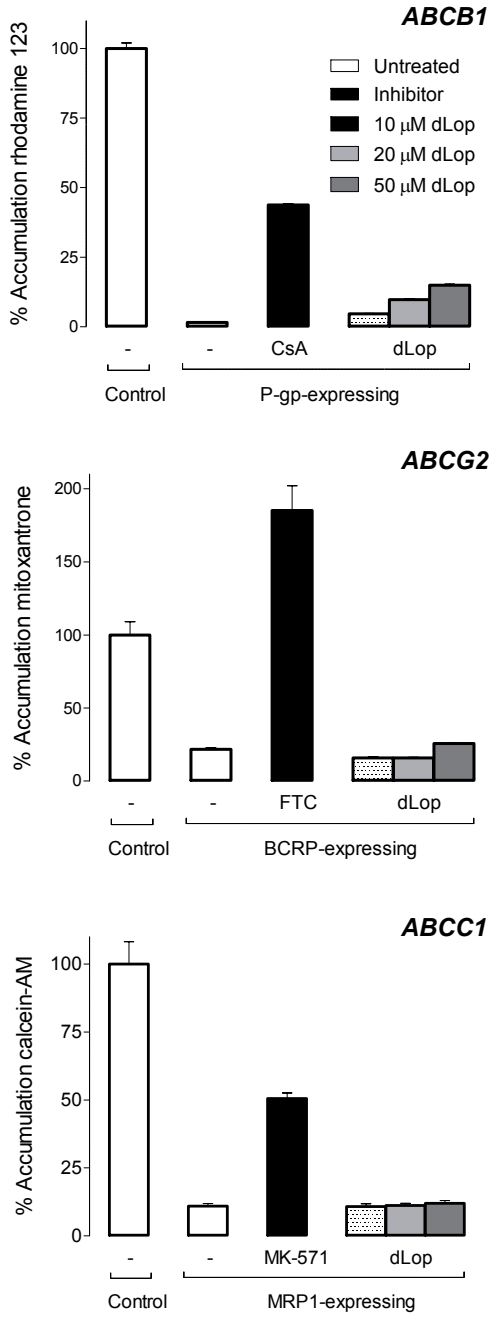

Figure 8. At micromolar concentrations, dLop behaves as a competitive substrate and inhibits the function of P-gp, but not of BCRP or MRP1. The cellular accumulation of transporter-specific fluorescent substrate is shown as a bar that represents the mean fluorescence intensity $\pm$ SD (n = 3) normalized to accumulation in untreated control cells. Fluorescent substrates and inhibitors with activity for each transporter were used. CsA (cyclosporin A, 10 μM), MK-571 (50 μM), FTC (fumitremorgin C, 5 μM).

In this study, both cultured human tumor cells and knockout mice were used to measure selectivity to isolate the interaction between the substrate and a single ABC transporter. This method is valuable for two reasons. First, to avoid confounding results from species differences [12], we assessed selectivity using human cell lines that overexpress each transporter. One limitation of these cells is that they are not polarized like the endothelial cells at the blood-brain barrier [107]. However, the cultured tumor cells offer a "cleaner" assessment of interaction between a drug and its transporter because polarized cell lines often express a high background of endogenous transporter expression [107], which can complicate the interpretation of substrate selectivity for a particular transporter. Therefore, human cells overexpressing a single ABC transporter were a better choice for the purposes of measuring selectivity in this study.

Second, the results from the in vitro system paralleled those found in the in vivo system. Imaging in knockout mice did not require ABC transporters to be inhibited by pharmacological agents, which are often not selective for a single ABC transporter [4, 75]. One limitation in our imaging studies, however, is that we did not measure the concentrations of the parent radioligand and radiometabolites in plasma of each mouse strain. It is possible that altered metabolism of [^{11}C]dLop made it appear that dLop is not a substrate for MRP1 or BCRP knockout mice, but this possibility is unlikely given that radiometabolism was similar in both P-gp knockout and wild-type mice [64] and that all the mice derive from the same genetic background.

In summary, our results show that, in both human and mouse tissues, dLop is selective for P-gp among the three efflux transporters of the blood-brain barrier, and that its activity is dependent on concentration. At low concentrations, dLop acts only as a substrate and at high concentrations, it acts as a

competitive substrate. Although high concentrations of dLop inhibit P-gp function, the low concentrations typically used for PET radiotracers would reflect substrate activity and not competitive inhibition of P-gp function.

4.1.2 dLop is ionically trapped in lysosomes (paper II)

The ionic trapping mechanism of dLop was measured as its accumulation in human KB-3-1 cells pretreated with compounds that raise lysosomal pH (Figure 9). Bafilomycin A, which prevents the acidification of the lysosomes by inhibiting the vacuolar proton ATPase pump [101], prevented [^{3}H]dLop accumulation in a dose-dependent manner. Similar results were obtained with tamoxifen, a weak base that raises lysosomal pH by depleting the free proton pool [102]. Accumulation of [^{3}H]dLop was also prevented by dLop itself.

Lysosomal competition of weak bases was also visualized using confocal microscopy (Figure 9). Control cells (KB-3-1) showed punctate red staining in the lysosomes from the fluorescent weak base LysoTracker Red DND-99 and blue staining in the nuclei from Hoechst 33342. LysoTracker staining decreased in cells treated with 100 μM dLop, a finding consistent with dLop displacing the lysosomal dye from lysosomes. A similar decrease was observed in cells that were treated with 100 μM of the weak base tamoxifen (positive control) but not in cells treated with 10 μM paclitaxel (negative control). These results support the hypothesis that the trapping of dLop in tissue is a result of accumulation of dLop as a protonated weak base within acidic lysosomes. Furthermore, the lysosomal trapping of dLop is consistent with that reported for other weak base P-gp substrates such as doxorubicin [108], daunomycin [109], and vinblastine [110].

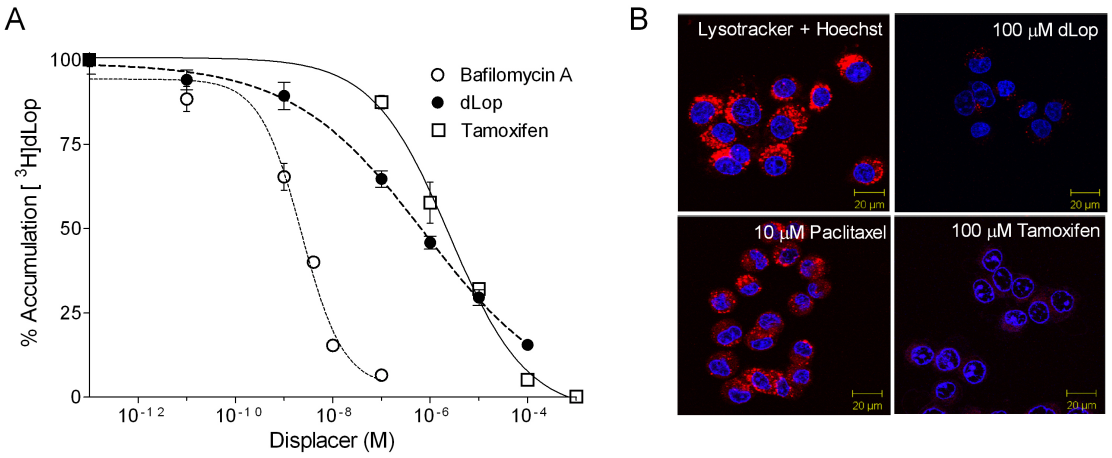

Figure 9. The P-gp substrate dLop is trapped in lysosomes. (A) Reduction of [^{3}H]dLop (1 nM) accumulation in control KB-3-1 cells by compounds that raise lysosomal pH. Data represent mean $\pm$ SD (n = 3). (B) Reduction in accumulation of a fluorescent weak base from lysosomes by dLop assessed by confocal microscopy. Images show the simultaneous staining of the lysosomes with LysoTracker Red DND-99 (10 nM) and of the nucleus with Hoechst 33342 (8 μM). dLop and tamoxifen (positive control) reduce the lysosomal staining, whereas paclitaxel (negative control) does not.

4.2 PROPERTIES OF TARIQUIDAR

4.2.1 Tariquidar competes with dLop for lysosomal accumulation in vitro and in vivo (paper II)

Since the in vivo trapping of [^{11}C]dLop in brain tissue was observed after P-gp inhibition, we measured [^{3}H]dLop uptake in control (KB-3-1) and P-gp-expressing cells (KB-8-5-11) treated with the P-gp inhibitor tariquidar. The inhibitor had two effects that were concentration-dependent in these two cell lines (Figure 10). At concentrations lower than 100 μM, tariquidar behaved as expected: it did not affect [^{3}H]dLop accumulation in control cells and increased accumulation in P-gp-expressing cells. However, at concentrations higher than 100 μM, tariquidar surprisingly decreased accumulation in both control and P-gp-expressing cells.

Since tariquidar decreased [^{3}H]dLop accumulation in control cells in a similar manner to weak bases, we investigated whether tariquidar itself is lysosomally trapped. Pretreatment of control cells (KB-3-1) with the weak bases tamoxifen and chloroquine decreased the cellular accumulation of [^{3}H]tariquidar. When combined together, these cell studies on tariquidar indicate that the compound has two behaviors: it inhibits P-gp and it is lysosomally trapped. Although the lysosomal trapping of tariquidar was not previously known, other P-gp inhibitors such as cyclosporin A [111] and verapamil [112] have been shown to interfere with the lysosomal sequestration of drugs.

We subsequently wondered whether lysosomal competition between tariquidar and dLop could occur in vivo because tariquidar is used with [^{11}C]dLop to image P-gp function in PET studies. We measured [^{11}C]dLop uptake in the presence and absence of tariquidar administration in lysosome-rich organs of P-gp knockout mice and healthy humans; P-gp knockout mice were used to examine the lysosomal effect of tariquidar without the confounding effect of P-gp inhibition. In P-gp knockout mice, radioactivity uptake was 35% ($P < 0.05$) lower in the kidneys and 40% ($P < 0.05$) lower in the spleens of tariquidar-

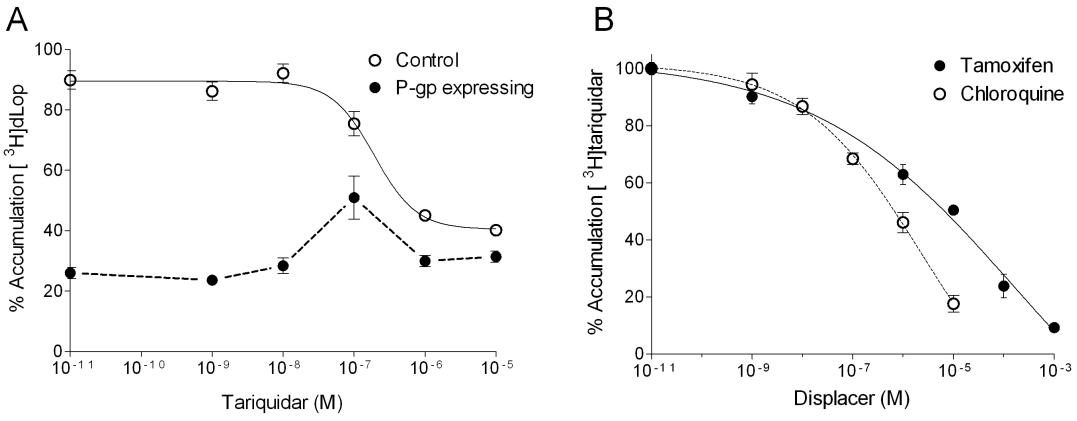

Figure 10. Tariquidar not only inhibits P-gp but is also lysosomally trapped in human cells. (A) Tariquidar has two effects on [^{3}H]dLop (1 nM) accumulation in control (KB-3-1) cells and in P-gp-expressing (KB-8-5-11) cells. At concentrations < 100 nM, tariquidar increases accumulation in P-gp-expressing cells while having no effect in control cells; at concentrations > 100 nM, tariquidar decreases accumulation in both cell lines. (B) Two weak bases, tamoxifen and chloroquine, decrease the cellular accumulation of [^{3}H]tariquidar (1 nM). Data represent mean $\pm$ SD (n = 3).

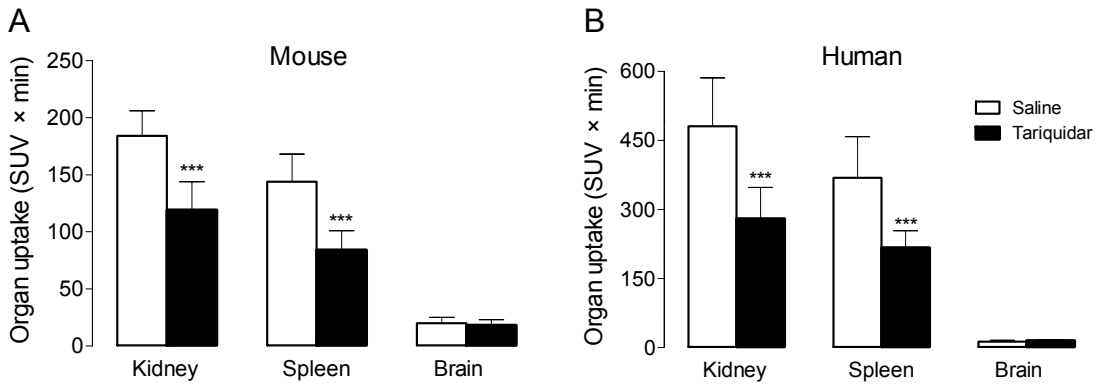

Figure 11. Uptake of radioactivity measured over 60 min in organs of P-gp knockout mice and from 5-120 min in organs of healthy humans after pretreatment with tariquidar and injection of [^{11}C]dLop. Pretreatment with tariquidar decreases [^{11}C]dlop accumulation in lysosome-rich organs (kidneys and spleen) but not in brain. Mice (n = 3 per treatment) were pretreated with tariquidar (32 mg/kg, i.v.) 30 min before injection of radiotracer and humans (n = 6) were pretreated with tariquidar (2 mg/kg, i.v.) immediately before injection of radiotracer ($P < 0.05$).

treated mice than that measured in saline-treated mice. Similarly, in humans, preinjection of tariquidar decreased radioactivity uptake in the kidneys by 41% ($P < 0.05$) and by 38% ($P < 0.05$) in the spleen compared with that measured at baseline conditions (Figure 11). The decrease was not not likely caused by a lower input function of [^{11}C]dLop because a previous study that used higher doses of tariquidar (4 mg/kg and 6 mg/kg i.v.) did not show a change in plasma concentration or protein binding of the parent radiotracer [88]. Although tariquidar is lysosomally trapped in these organs, it still acts as an inhibitor of P-gp, as demonstrated by a 71% ($P < 0.05$) and 66% ($P < 0.05$) decrease in radioactivity excretion into the bladder and gallbladder, respectively.

Unlike the competition observed in the peripheral organs, lysosomal competition between tariquidar and [^{11}C]dLop was not observed in the brains of mice or humans using PET. Recent studies indicate that tariquidar does not enter the rodent brain [60, 62], meaning that tariquidar could not compete with the lysosomal trapping of [^{11}C]dLop in the brain in vivo. However, using confocal microscopy, we confirmed that tariquidar does compete for lysosomes in isolated rat neurons in which the blood-brain barrier is not functional.

In summary, the P-gp inhibitor tariquidar is trapped in lysosomes and competes with dLop for accumulation in lysosomes. How do the two properties of tariquidar – lysosomal trapping and P-gp inhibition – affect in vivo studies measuring P-gp function with [^{11}C]dLop? In the periphery, tariquidar competes for lysosomes with [^{11}C]dLop (as seen in the kidneys and spleen) but also inhibits P-gp (as seen in the bladder and gallbladder); therefore, these competing interactions would complicate the measurement of P-gp function in the periphery. At the blood-brain barrier, however, tariquidar only inhibits P-gp because it cannot enter the brain to compete lysosomally; therefore, the inhibitor can still be used with [^{11}C]dLop to measure P-gp function at the blood-brain barrier.

4.2.2 Tariquidar is not a selective inhibitor of P-gp (paper III)

As mentioned in the above section, when [^{11}C]tariquidar was injected in wild-type mice, the amount of radioactivity detected in the brain was negligible [60, 62]. The radiotracer

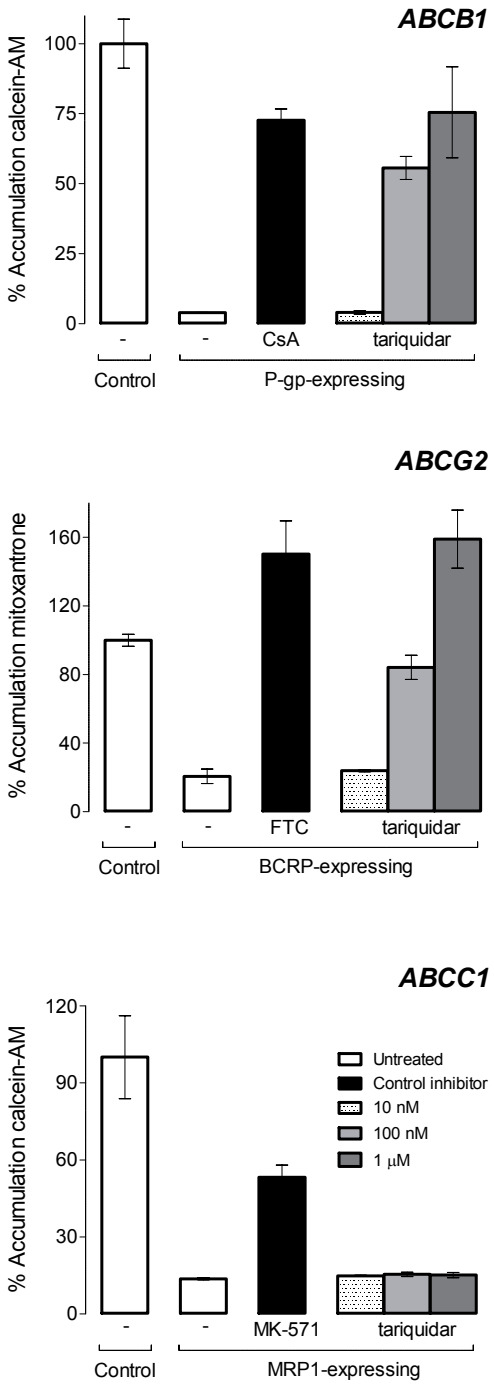

Figure 12. Tariquidar inhibits the function of P-gp and BCRP but not MRP1. The cellular accumulation of transporter-specific fluorescent substrate is shown as a bar that represents the mean fluorescence intensity ± SD (n = 3) normalized to accumulation in untreated control cells. Fluorescent substrates and inhibitors with activity for each transporter were used. CsA (cyclosporin A, 10 μM), MK-571 (50 μM), FTC (fumitremorgin C, 5 μM).

also had negligible binding in brains of P-gp and BCRP knockout mice, but had detectable binding in brains of dual P-gp/BCRP knockout mice [60, 62]. Because these results were not straightforward, we sought to determine the selectivity of tariquidar as a inhibitor and a substrate for P-gp, MRP1 and BCRP.

The selectivity of tariquidar as an inhibitor for each transporter was measured by its ability to inhibit the efflux of a fluorescent substrate. Compared to untreated transporter-expressing cells, P-gp- and BCRP-expressing cells treated with $\geq$ 100 nM tariquidar had 14-fold ($P < 0.001$) and 4-fold ($P < 0.001$) higher uptake of a fluorescent substrate, respectively (Figure 12). These data indicate that tariquidar inhibits both transporters with similar potency because at 100 nM, it restored accumulation to 56% of control for P-gp and 84% of control for BCRP, although the potency of tariquidar to block P-gp and BCRP in vivo may vary according to expression levels. The inhibition data for P-gp cells are consistent with results from Callaghan and colleagues [46]. Tariquidar did not increase accumulation of substrate in MRP1-expressing cells (Figure 12). As positive controls, inhibition of each transporter was demonstrated with a known inhibitor.

The selectivity of tariquidar as a substrate for each transporter was measured as the accumulation of [^{3}H]tariquidar at low concentrations (1 nM) in three pairs of cell lines. Control cells of the ABCG2 pair accumulated 4 times more [^{3}H]tariquidar than BCRP-expressing cells ($P < 0.001$). Because these results indicate that tariquidar is a BCRP substrate, we used an ATPase assay to investigate whether tariquidar stimulates ATPase activity of the BCRP transporter. We found a 2.5-fold increase in ATPase activity from basal levels, and the concentration required for 50% stimulation of ATP hydrolysis was 138.14 ± 21.4 nM (Figure 13). Tariquidar's affinity for BCRP is similar to other avid substrates of

BCRP [113] and corresponds well with its activity as a competitive substrate of BCRP because tariquidar inhibits P-gp as a pure inhibitor at a much lower affinity (5.1 nM) [46].

In contrast to the findings in the ABCG2 pair, tariquidar was not found to be a substrate in the ABCB1 or ABCC1 pairs (Figure 13). In the ABCB1 pair, tariquidar had a 2-fold higher "accumulation" in P-gp-expressing cells than in control cells ($P < 0.001$), suggesting that tariquidar is actually binding to P-gp. In the ABCC1 pair, accumulation between control and MRP1-expressing cells was not different ($P = 0.16$), suggesting no interaction with the MRP1 transporter. An interesting observation is that while tariquidar binds to P-gp at a low concentration (1 nM), it does not inhibit transporter function as observed in the fluorescence efflux assay. For partial inhibition of P-gp function in human cells, > 10 nM tariquidar is required (Figure 10). A likely explanation for this phenomenon is the presence of "spare receptors", where a sizable percentage of transporter must be blocked before loss of function is observed. In brief, P-gp works so rapidly and with such high capacity that even when a sizable percentage of transporters is blocked (e.g. 60-80%), the remaining functional transporter (20-40%) can still effectively preclude entry of substrate [114].

In sum, tariquidar interacts with P-gp as an inhibitor and with BCRP as a competitive substrate. At low concentrations (1 nM), tariquidar binds to P-gp and is effluxed by BCRP, but at higher concentrations ($\geq$ 100 nM), it inhibits the function of both P-gp and BCRP. In clinical studies of P-gp inhibition, tariquidar has generally been administered at a dose of 2 mg/kg i.v., which results in a plasma concentration of 2.3 μM [93]. Although tariquidar would be able to inhibit both P-gp and BCRP at this dose, the net in vivo effects of tariquidar will depend not only on its concentration but also on the concentrations of P-gp and BCRP.

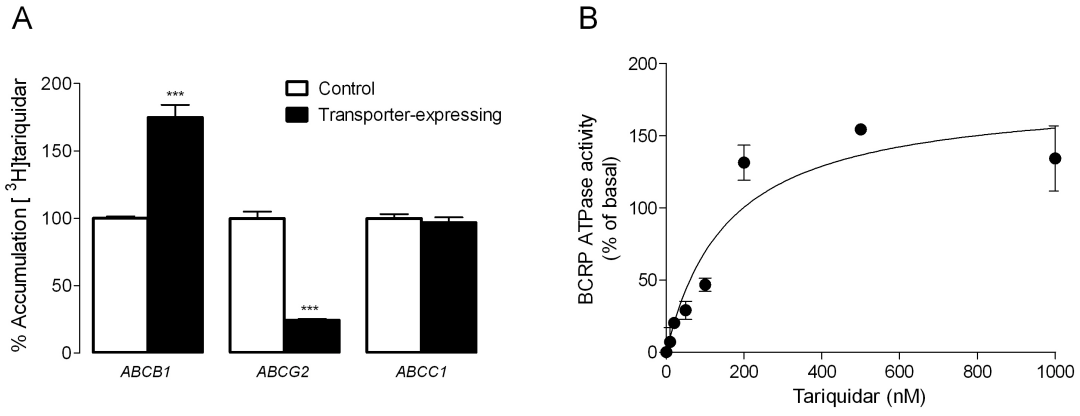

Figure 13. The selectivity of tariquidar as a substrate for three ABC transporters measured in human cell lines and BCRP-expressing vesicles. (A) [^{3}H]tariquidar accumulation is 4-fold higher in control cells than in BCRP-expressing cells, but is 2-fold higher in P-gp-expressing cells than in control cells. Bars represent mean $\pm$ SD (n = 6). (B) Tariquidar stimulates ATPase activity to 2.5-fold the basal activity, demonstrating a direct substrate interaction with BCRP (concentration required for 50% stimulation = 138.4 $\pm$ 21.4 nM). The basal activity was subtracted to calculate percent stimulation in the presence of indicated concentrations of tariquidar. Data points represent mean $\pm$ SD (n = 3).

4.2.3 Tariquidar is not useful for measuring P-gp density at the BBB

Given that our results indicate that tariquidar binds to P-gp at low concentrations (1 nM), why did PET studies using [^{11}C]tariquidar result in no signal in the mouse brain in vivo [60, 62]? One explanation for the low in vivo signal is that [^{11}C]tariquidar may be pumped out by BCRP in the endothelial cells of the blood-brain barrier before it has a chance to bind to P-gp. However, because [^{11}C]tariquidar had a negligible brain signal in BCRP knockout mice, which still express P-gp, this possibility is unlikely [60, 62]. Another explanation is that the binding potential of P-gp and tariquidar is too low to be visualized using PET, where the binding potential is the product of receptor density (B_{max}) and affinity ($1/K_D$) of the radioligand. The cross reactivity of tariquidar to BCRP and the low PET signal reported in mouse brain suggest that this inhibitor may not be a useful radiotracer to measure P-gp density in vivo.

Since our goal is to be able to measure P-gp density levels in brain, we assessed the technique of autoradiography instead to visualize P-gp density. As with PET, this technique allows the spatial distribution and density of receptors to be measured in tissue slices [100]. We first confirmed that [^{3}H]tariquidar actually binds to mouse P-gp, since all our previous binding studies with tariquidar were performed in human cells. P-gp expressing cells from the mouse NIH-C3M line (91.8 $\pm$ 8.9 fmol/10^6 cells) bound 2 times more [^{3}H]tariquidar than control NIH-3T3 cells (40.2 $\pm$ 2.7 fmol/10^6 cells; $P < 0.01$), similar to the binding observed in human cells (Figure 13). These results indicate that 1 nM tariquidar does bind to mouse P-gp.

Binding of [^{3}H]tariquidar to P-gp at the blood-brain barrier was then measured as the amount of radioactivity per unit area in brain slices of wild-type and P-gp knockout mice. The time required for binding to reach equilibrium was $\geq$ 120 min at 22 °C measured in wild-type brain slices. Binding of [^{3}H]tariquidar was 27% $\pm$ 11% ($P < 0.01$) lower in P-gp knockout mice than in wild-type mice, which could indicate the specific binding of tariquidar to P-gp (Figure 14). Furthermore, in brains of wild-type mice, [^{3}H]tariquidar binding was displaced by a maximum of 30 $\pm$ 9% ($P < 0.05$) using $\leq$ 10 μM and by 64% ($P < 0.001$) using 50 μM unlabeled tariquidar. However, in brains of P-gp knockout mice, [^{3}H]tariquidar binding was also displaced by 20 $\pm$ 5% ($P < 0.05$) using $\leq$ 10 μM unlabeled tariquidar and by 53% ($P < 0.001$) using 50 μM unlabeled tariquidar (Figure 14). Displacement of binding in P-gp knockout mice suggests that tariquidar has a specific binding site other than P-gp because non-specific binding is considered nondisplaceable [59].

To determine whether this second binding site was unique to tariquidar, we performed similar displacement studies using the P-gp inhibitor cyclosporin A. We found that cyclosporin A did not significantly reduce the binding of [^{3}H]tariquidar in either wild-type or P-gp knockout mice (Figure 14), a finding that further supports the idea of an additional binding site specific to tariquidar.

Although the results from the cell and autoradiography studies indicate that tariquidar's binding to P-gp can be measured, the autoradiography results demonstrate that the specific-to-nonspecific (i.e. signal-to-noise) ratio is low. That is, the signal from tariquidar binding to P-gp (20-30% of the total signal) is much lower than the signal from tariquidar binding to non-P-gp sites (70-80% of the total signal) in brain tissue. The range of specific binding signal measured in our studies is about 10-20% lower than that published by Bauer and colleagues [62]. One explanation for this difference is that they performed their binding studies with [^{11}C]tariquidar for 30 min [62], a time range that may not re-

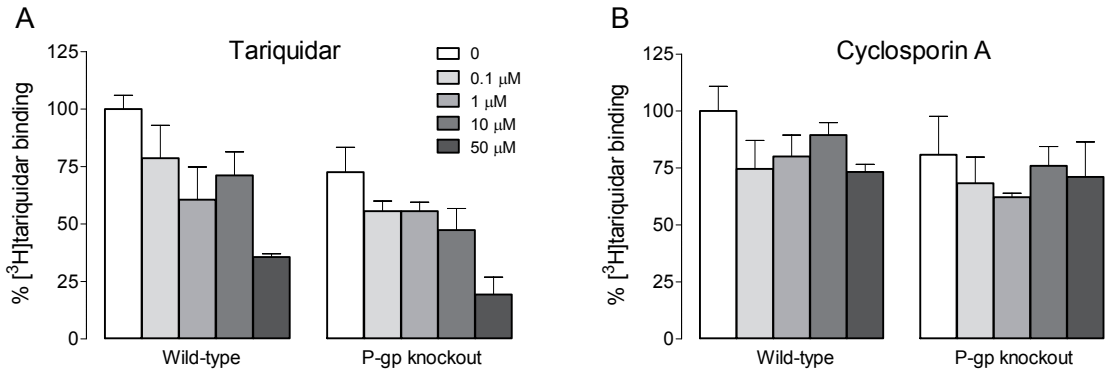

Figure 14. P-gp density measured as the binding of [^{3}H]tariquidar in wild-type and P-gp knockout mouse brains at 22 °C. (A) In both strains of mice, ≤ 10 μM of unlabeled tariquidar displaces [^{3}H]tariquidar binding by 20-30% and 50 μM unlabeled tariquidar displaces binding by about 50-60%. (B) In both strains of mice, all concentrations of the P-gp inhibitor cyclosporin A displace [^{3}H]tariquidar binding by 20-30%. Data represent mean $\pm$ SD (n = 3).

flect equilibrium, as we found that [^{3}H]tariquidar binding reached equilibrium at 120 min. Another interesting observation is that while the signal from tariquidar binding to P-gp is low in both autoradiography and PET, the signal from the binding of tariquidar to non-P-gp sites ("noise") in brain tissue is measurable by autoradiography but not by PET. We speculate that this "noise" cannot be measured by PET because tariquidar cannot cross the blood-brain barrier to bind to the other sites in brain tissue.

The low signal-to-noise ratio measured in autoradiography supports the idea that the binding of tariquidar to P-gp is too low to measure, both in brain slices and in the living brain. Kamiie and colleagues determined that P-gp density in endothelial cells from mouse brain capillaries is 15 fmol/μg protein [115], which translates to a value of 3 nM assuming that the brain endothelial volume is 0.2% of total brain [116]. Assuming that the K_D (the reciprocal of affinity) of tariquidar for P-gp is 5.1 nM [46], the binding potential (the product of density and affinity) for tariquidar and P-gp is estimated to be 0.59, well below the suggested value of 10 for PET imaging [117]. This binding potential would be even lower in humans, as Kamiie and colleagues recently reported a P-gp density of 6.06 fmol/μg protein [118].

In summary, tariquidar is not a useful compound for measuring P-gp density at the blood-brain barrier because of its multiple specific binding sites and low signal-to-noise ratio. Given the density of P-gp at the blood-brain barrier, PET and autoradiography measurements of density may require a compound with a higher affinity (at least high picomolar) for P-gp.

5 CONCLUSIONS

The focus of this thesis was to determine the pharmacological properties of two radiotracers that measure P-gp function and density using in vitro and in vivo methods.

We found that the radiotracer [^{11}C]dLop is a substrate selective for P-gp among the three most common ABC transporters (P-gp, BCRP, and MRP1) of the blood-brain barrier. The compound is also ionically trapped in acidic lysosomes, a mechanism that increases it signal-to-noise ratio in PET imaging. These two favorable properties – selectivity and high signal strength – indicate that dLop can specifically image P-gp function at the blood-brain barrier using PET. However, [^{11}C]dLop and tariquidar cannot be used together to measure P-gp function in the periphery because tariquidar competes with dLop for accumulation in lysosomes of peripheral organs of the body.

In contrast, the radiotracer [^{11}C]tariquidar is not selective for P-gp, as it has substrate activity for the BCRP transporter. The compound also cannot measure P-gp density at the blood-brain barrier because of its low signal-to-noise ratio. Because the density of P-gp at the blood-brain barrier is low, measurement of density may require a compound with higher affinity for P-gp.

6 FUTURE PERSPECTIVES

Development of substrate radioligands that are weak P-gp substrates. [^{11}C]dLop is a promising radiotracer to selectively image the function of P-gp at the BBB because it is selective for P-gp, has a high signal strength, and has a pure radiochemical signal. Although it fulfills the three criteria for an ideal substrate radioligand, its application is limited because it is an extremely avid substrate for P-gp. [^{11}C]dLop would be useful for measuring P-gp function in disorders where function is reduced, because it would rapidly enter the brain and have a strong signal. However, [^{11}C]dLop would not be useful in measuring P-gp function in disorders where function is increased, because the brain uptake of [^{11}C]dLop at baseline is extremely low. In contrast, a substrate radiotracer that is a weaker substrate of P-gp might be capable of measuring increased P-gp function because it would have moderate brain uptake at baseline conditions [119]. Further studies are required to determine the utility of weak base substrates in conditions of increased P-gp function.

Development of substrate radioligands to measure P-gp function in the periphery. As demonstrated in this thesis, the competitive interaction of [^{11}C]dLop and tariquidar in lysosomes is problematic for measuring P-gp function in the periphery. [^{94m}Tc]Sestamibi and [^{68}Ga]ENBPI are two metal complex radiotracers that have the potential for imaging P-gp function in the periphery because they become trapped in mitochondria [120] and would therefore not compete for lysosomal accumulation with tariquidar. However, both these tracers show substrate activity in vitro for MRP1 [78, 121] and this cross-reactivity might limit the selective quantification of P-gp in vivo. New substrate radioligands, such as [^{11}C]MC266 [122], have been developed and evaluated, but future work needs to ensure that these new compounds are selective for P-gp, have high signal strength, and do not interfere with the lysosomal trapping of tariquidar.

Development of inhibitor radioligands with higher affinity for P-gp. Although [^{11}C]tariquidar is one of the highest affinity P-gp inhibitors available, the radiotracer cannot measure P-gp density in vivo because the binding potential (product of receptor density and affinity) of P-gp and tariquidar is estimated to be 0.59 in mice and 0.24 in humans. In order to have a high enough (a binding potential > 10) signal in vivo [117], future inhibitors used to measure P-gp density may need to have a 10-fold higher affinity than tariquidar for imaging in mice and a 50-fold higher affinity than tariquidar for imaging in humans. Even though its affinity is undetermined, a new inhibitor radioligand [^{11}C]MC18 demonstrates that P-gp density can be imaged in vivo because the radiotracer had measurable brain binding at baseline and 30% lower binding after P-gp inhibition. However, because the ratio of specific to nonspecific binding for this compound is low (i.e. 70% of the signal was nondisplaceable), more work is needed to improve the specificity and affinity of inhibitor radiotracers used to image P-gp density.

Radioligands to measure the function and density of other ABC transporters. Many of the PET studies on ABC transporters have focused on imaging P-gp function and density, but recent research has indicated that BCRP may be an important transporter to study because its density is higher than that of P-gp in humans [118]. As such, substrates and inhibitors of BCRP are being screened and developed for PET imaging [123, 124]. Fur-

thermore, work is also being done on candidate radioligands for imaging MRP1 function at the BBB [125].

7 ACKNOWLEDGEMENTS

Wow! The past few years have been an incredible, fulfilling experience that would not have been possible without the scientific contribution and support of many people. I would like to thank the National Institutes of Health (NIH) and Karolinska Institutet (KI) for funding the research in this thesis, and express my deepest gratitude to the following people:

Christer Halldin, my KI supervisor, for giving me freedom to develop my own projects and initiating thought-provoking discussions that guided my work at Karolinska. Your optimism and enthusiasm for science are contagious!

Robert Innis, my NIH co-supervisor, who taught me the art of critical scientific thinking, writing, presenting, and designing experiments. Your analytical skills and knowledge of pharmacology guided my projects and will continue to do so in the future.

Matthew Hall, my NIH co-supervisor, for training me in molecular biology techniques and for being an endless source of ideas, support, and advice. Your friendship, shared love of coffee, and humor allowed me to tackle science, especially during difficult times. I still have that energy chart you drew for me on my first day of lab to remind me of the important things in life!

Sharon Milgram, my mentor, for being one of my biggest cheerleaders, voice of reason, and a fantastic role model.

All former and current members of the Molecular Imaging Branch at the National Institute of Mental Health. *Elizabeth Alzona* for your enormous patience, support, and ability to navigate the maze of paperwork at NIH. *Sami Zoghbi*, who helped me become an organized and meticulous scientist. From botany to the chemistry of food, your application and knowledge of science to everyday life were always appreciated (and educational)! *Jeih-San*, for teaching me everything I know about rodent PET imaging. *Victor Pike*, whose pointed questions challenged me to improve my science and learn more about chemistry! *Saurav Shrestha*, whose social spirit and energy was always welcome in daily life. *Garth Terry*, *Nick Seneca*, and *Mette Skinbjerg*, for being great role models to follow in the NIH/KI program. *Chuck Kreisl*, *Jussi Hirvonen*, *Christina Hines, Masahiro Fujita, Yasuyuki and Nobuyo Kimura*, and *Talakad Lohith*, who were great company in lab and at scientific conferences. *Robert Gladding*, for your stand-up comedy. *Kacey Anderson*, *Kimberly Jenko*, *Edward Tuan*, *Amanda Farris*, and *Leah Dickstein*, for great teamwork in lab and friendship outside of lab. *Cheryl Morse*, *Jinsoo Hong*, *Fabrice Simeon*, *Shuiyu Lu, Umesha Shetty*, *Andrew Taku*, *Kelly Sprague*, *Yi Zhang*, and *Sanjay Telu*, for your excellent chemistry skills and synthesis of radiolabeled compounds, sometimes at last minute. *Desiree Ferraris Araneta*, and *Gerald Hodges* for helping coordinate the human studies.

Members of the Laboratory of Cell Biology at the National Cancer Institute. *Michael Gottesman*, who always took time from a busy schedule to ask about my research and well-being. *Kyle Brimacombe*, for help with navigating the cell culture lab and teaching me how to interpret flow cytometry graphs! *Kristy Pluchino*, *Suneet Shukla*, *Andrew Goldsborough*, and *Paul Lund*, for making lab work entertaining. *George Leiman*, *Barbara Murphy*, *Suresh Ambudkar*, *Ding-Wu Shen*, *Carol Cardelli*, and *Susan Garfield* for assistance in various technical and scientific matters.

Members of the Section of Psychiatry and Science for Life at Karolinska Institutet. Jag kände mig välkommen i Sverige tack vare er alla! *Karin Zahir* och *Marianne Youssefi*, tack för era hjälp med alla administrativa saker och *Karin*, tack för att du pratat svenska med mig! *Siv Eriksson* för din vänlighet och för att du tränat mig på olika tekniker i labbet. *Balázs Gulyás*, whose knowledge of neurobiology steered my research in the right directions. *Zhisheng Jia*, for synthesizing and purifying radiolabeled compounds for me. *Jan Mulder*, who kindly adopted me into his lab and shared his vast knowledge of techniques of protein detection with me. *Tony Beristain*, for reminding me that objectivity in science died a long time ago. *Martin Schain*, for your generosity over the years. I will never forget the bathtub model for convolutions! If you become famous, just remember to keep it real, homie. *Miklós Toth*, for fun biology-oriented discussions and help with my imaging software. *Jenny Häggkvist*, for all your PhD/career-related advice and for being a great sound board for ideas. *Magdalena Nord* for introducing me to Lindy Hop, which became one of my favorite pastimes! *Mahabuba Jahan*, *Sangram Nag*, *Anton Forsberg*, *Mikael Tiger, Johan Lundberg*, *Janine Doordin*, *Kalman Nagy*, *Roman Krais*, *Shigeyuki Yamamoto* and *Granville Matheson*, for entertaining lunch discussions ranging from the biology of plants to etymology. *Sjoerd Finnema*, for great conversations about life as a scientist and tolerating all my PhD and career-related questions. *Urban Hansson*, who gets endless thanks for recovering the hard disk containing my PhD work! *Andrea Varrone*, for nice discussions on PET modeling and running marathons. *Gudrun Nylen*, *Pia Schönbeck* och *Sophia Sjödin*, för att vara trevliga arbetskamrater! Other colleagues for making the work environment more enjoyable: *Vladimir Stepanov, Anna Sumic, Katarina Varnäs, Akihiro Takano, Ryuji Nakao, Magnus Schou, Carsten Steiger, Guennadi Jogolev, Kenneth Dahl, Lars Farde, Simon Cervenka, Jacqueline Borg, Linda Bergman, Jan Andersson, Per Kalsson*, and *Arsalan Amir*.

Members of the Office of Intramural Research and Education. *Philip Wang*, *Betsey Wagener*, and *Caroline Duffy*, whose cheerful personalities and friendship always brightened my day! Your support and advice helped me get through difficult times. *Lori Conlan*, *Elaine Diggs*, and *Bill Higgins*, whose career advice was always honest and profound. *Barbara Ward*, for always getting me onto Sharon's schedule when I needed it the most!

To my wonderful friends, *Katie, Pavithra, Ivana, Rebecca and Anna*, you are all incredible women and an inspiration to me! Thanks for reminding me that there is a life outside of lab and for staying in touch, regardless of the distance. *Vania*, best co-chair and friend in grad school! Our shared love of improv singing, art and food made spending time with you so much fun. May you find illumination both in science and life. :) *Erik*, for your meaningful friendship and for keeping in touch, despite your busy schedule. You are going to be such a great doctor! *Tracy, Daniela, Eva, Maggie, Ivy, Rezin, Miriam*, the best travel buddies I could ask for! We had fun trips, excellent dinners, and great memories in Sweden. *Niko*, how fantastic is it that we managed to be neighbors in two countries? I really enjoy our lunch conversations about life, bureaucracy, and the politics of science. *David*, my favorite Lindy Hop partner! *Jonas* et *Frédéric*, merci pour la relecture du texte français. *Augustin, Kate, Tracy Jill, Kim, Alexis, Chris, Allison, Dan, Erica*, for helping me find my social niche at the NIH. Members of the NIH acapella group: thanks for the great singing memories.

To my amazing family, *Amma*, *Appa*, and *Pallavi*. Thanks for always believing in me

and for your endless love. Without your support, I wouldn't have come this far. À *Pauline* et *Soizick*, ma famille française à qui je tiens. To *Barty, Clemens, Linda,* and *Christian* for welcoming me in your family.

À mon amour, *Winni*. Merci pour ton soutien precieux durant ces années et pour avoir toujours réussi à me faire rire. Malgré la distance qui nous sépare, tu es toujours avec moi. Je te promets d'apprendre l'allemand un jour. :)

8 REFERENCES

[1] Alberts, B. *et al. Molecular Biology of the Cell* (Garland Science, New York, 2002).

[2] Dean, M., Rzhetsky, A. & Allikmets, R. The human ATP-binding cassette (ABC) transporter superfamily. *Genome Res.* **11**, 1156–66 (2001).

[3] Gottesman, M. Mechanisms of cancer drug resistance. *Annu. Rev. Med.* **53**, 615–27 (2002).

[4] Szakács, G., Paterson, J., Ludwig, J., Booth-Genthe, C. & Gottesman, M. Targeting multidrug resistance in cancer. *Nat. Rev. Drug Disc.* **5**, 219–34 (2006).

[5] Dantzig, A., de Alwis, D. & Burgess, M. Considerations in the design and development of transport inhibitors as adjuncts to drug therapy. *Adv. Drug Deliver. Rev.* **55**, 133–50 (2003).

[6] Bredel, M. Anticancer drug resistance in primary human brain tumors. *Brain Res.* **35**, 161–204 (2001).

[7] Ambudkar, S. *et al.* Biochemical, cellular, and pharmacological aspects of the multidrug transporter. *Annu. Rev. Pharmacol. Toxicol.* **39**, 361–98 (1999).

[8] Higgins, C., Callaghan, R., Linton, K., Rosenberg, M. & Ford, R. Structure of the multidrug resistance P-glycoprotein. *Semin. Cancer Biol.* **8**, 135–142 (1997).

[9] Rosenberg, M., Callaghan, R., Ford, R. & Higgins, C. Structure of the multidrug resistance P-glycoprotein to 2.5 nm resolution determined by electron microscopy and image analysis. *J. Biol. Chem.* **272**, 10685–10694 (1997).

[10] Aller, S. *et al.* Structure of P-glycoprotein reveals a molecular basis for poly-specific drug binding. *Science* **323**, 1718–1722 (2009).

[11] Gottesman, M., Fojo, T. & Bates, S. Multidrug resistance in cancer: role of ATP-dependent transporters. *Nat. Rev. Cancer* **2**, 48–58 (2002).

[12] Syvänen, S. *et al.* Species differences in blood-brain barrier transport of three positron emission tomography radioligands with emphasis on P-glycoprotein transport. *Drug Metab. Disp.* **37**, 635–43 (2009).

[13] Graff, C. & Pollack, G. Drug transport at the blood-brain barrier and the choroid plexus. *Curr. Drug Metab.* **5**, 95–108 (2004).

[14] Cordon-Cardo, C. *et al.* Expression of the multidrug resistance gene product (P-glycoprotein) in human normal and tumor tissues. *J. Histochem. Cytochem.* **38**, 1277–1287 (1990).

[15] Thiebaut, F. *et al.* Cellular localization of the multidrug-resistance gene product P-glycoprotein in normal human tissues. *Proc. Natl. Acad. Sci. U.S.A* **84**, 7735–7738 (1987).

[16] Chandra, P. & Brouwer, K. The complexities of hepatic drug transport: current knowledge and emerging concepts. *Pharm. Res.* **21**, 719–735 (2004).

[17] Ros, J. *et al.* ATP binding cassette transporter gene expression in rat liver progenitor cells. *Gut* **52**, 1060–1067 (2003).

[18] Dombrowski, S. *et al.* Overexpression of multiple drug resistance genes in endothelial cells from patients with refractory epilepsy. *Epilepsia* **42**, 1501–6 (2001).

[19] Golden, P. & Pardridge, W. P-glycoprotein on astrocyte foot processes of unfixed isolated human brain capillaries. *Brain Res.* **819**, 143–6 (1999).

[20] Melaine, N. *et al.* Multidrug resistance genes and P-glycoprotein in the testis of the rat, mouse, Guinea pig, and human. *Biol. Reprod.* **67**, 1699–1707 (2002).

[21] Tribull, T., Bruner, R. & Bain, L. The multidrug resistance-associated protein 1 transports methoxychlor and protects the seminiferous epithelium from injury. *Toxicol. Lett.* **142**, 61–70 (2003).

[22] Atkinson, D., Greenwood, S., Sibley, C., Glazier, J. & Fairbairn, L. Role of MDR1 and MRP1 in trophoblast cells, elucidated using retroviral gene transfer. *Am. J. Physiol. Cell Physiol.* **285**, C584–C591 (2003).

[23] St-Pierre, M. *et al.* Expression of members of the multidrug resistance protein family in human term placenta. *Am. J. Physiol.- Reg. I.* **279**, R1495–R1503 (2000).

[24] Schinkel, A. P-glycoprotein, a gatekeeper in the blood-brain barrier. *Adv. Drug Deliver. Rev.* **36**, 179–194 (1999).

[25] Zhou, S. Structure, function and regulation of P-glycoprotein and its clinical relevance in drug disposition. *Xenobiotica* **38**, 802–832 (2008).

[26] Kimchi-Sarfaty, C. *et al.* A "silent" polymorphism in the MDR1 gene changes substrate specificity. *Science* **315**, 525–8 (2007).

[27] Gréen, H., Söderkvist, P., Rosenberg, P., Horvath, G. & Peterson, C. ABCB1 G1199A polymorphism and ovarian cancer response to paclitaxel. *J. Pharm. Sci.* **97**, 2045–2048 (2008).

[28] Miyake, K. *et al.* Molecular cloning of cDNAs which are highly overexpressed in mitoxantrone-resistant cells: demonstration of homology to ABC transport genes. *Cancer Res.* **59**, 8–13 (1999).

[29] Doyle, L. *et al.* A multidrug resistance transporter from human MCF-7 breast cancer cells. *Proc. Natl. Acad. Sci. U.S.A* **95**, 15665–15670 (1998).

[30] Allikmets, R., Schriml, L., Hutchinson, A., Romano-Spica, V. & Dean, M. A human placenta-specific ATP-binding cassette gene (ABCP) on chromosome 4q22 that is involved in multidrug resistance. *Cancer Res.* **58**, 5337–5339 (1998).

[31] Polgar, O., Robey, R. & Bates, S. ABCG2: structure, function and role in drug response. *Exp. Drug Opin. Metab. Toxicol.* **4**, 1–15 (2008).

[32] McDevitt, C. *et al.* Purification and 3D structural analysis of oligomeric human multidrug transporter ABCG2. *Structure* **14**, 1623–32 (2006).

[33] Xu, J., Liu, Y., Yang, Y., Bates, S. & Zhang, J.-T. Characterization of oligomeric human half-ABC transporter ATP-binding cassette G2. *J. Biol. Chem.* **279**, 19781–9 (2004).

[34] Cooray, H., Blackmore, C., Maskell, L. & Barrand, M. Localisation of breast cancer resistance protein in microvessel endothelium of human brain. *NeuroReport* **13**, 2059–2063 (2002).

[35] Naomi, M. *et al.* Impaired renal excretion of 6-hydroxy-5,7-dimethyl-2-methylamino-4-(3-pyridylmethyl)benzothiazole (E3040) sulfate in breast cancer resistance protein (BCRP1/ABCG2) knockout mice. *Drug Metab. Disp.* **32**, 898–901 (2004).

[36] Maliepaard, M. *et al.* Subcellular localization and distribution of the breast cancer resistance protein transporter in normal human tissues. *Cancer Res.* **61**, 3458–3464 (2001).

[37] Jonker, J. *et al.* Role of breast cancer resistance protein in the bioavailability and fetal penetration of topotecan. *J. Natl. Cancer Inst.* **92**, 1651–1656 (2000).

[38] Jonker, J. *et al.* The breast cancer resistance protein BCRP (ABCG2) concentrates drugs and carcinogenic xenotoxins into milk. *Nature Med.* **11**, 127–129 (2005).

[39] Zhou, S. *et al.* The ABC transporter Bcrp1/ABCG2 is expressed in a wide variety of stem cells and is a molecular determinant of the side-population phenotype. *Nature Med.* **7**, 1028–1034 (2001).

[40] Rosenberg, M. *et al.* The structure of the multidrug resistance protein 1 (MRP1/ABCC1). crystallization and single-particle analysis. *J. Biol. Chem.* **276**, 16076–82 (2001).

[41] Cole, S. & Deeley, R. Transport of glutathione and glutathione conjugates by MRP1. *Trends Pharmacol. Sci.* **27**, 438–46 (2006).

[42] Sugiyama, D., Kusuhara, H., Lee, Y.-J. & Sugiyama, Y. Involvement of multidrug resistance associated protein 1 (Mrp1) in the efflux transport of 17beta estradiol-D-17beta-glucuronide (E217betaG) across the blood-brain barrier. *Brain* **20**, 1394–1400 (2003).

[43] Zhang, Y., Schuetz, J., Elmquist, W. & Miller, D. Plasma membrane localization of multidrug resistance-associated protein homologs in brain capillary endothelial cells. *J. Pharmacol. Exp. Ther.* **311**, 449–455 (2004).

[44] Ros, J., Libbrecht, L., Geuken, M., Jansen, P. & Roskams, T. High expression of MDR1, MRP1, and MRP3 in the hepatic progenitor cell compartment and hepatocytes in severe human liver disease. *J. Pathol.* **200**, 553–560 (2003).

[45] Peng, K. *et al.* Tissue and cell distribution of the multidrug resistance-associated protein (MRP) in mouse intestine and kidney. *J. Histochem. Cytochem.* **47**, 757–68 (1999).

[46] Martin, C. *et al.* The molecular interaction of the high affinity reversal agent XR9576 with P-glycoprotein. *Br. J. Pharmacol.* **128**, 403–411 (1999).

[47] Calcagno, A., Kim, I., Wu, C., Shukla, S. & Ambudkar, S. ABC drug transporters as molecular targets for the prevention of multidrug resistance and drug-drug interactions. *Curr. Drug Deliv.* **4**, 324–33 (2007).

[48] Pauli-Magnus, C. *et al.* Characterization of the major metabolites of verapamil as substrates and inhibitors of P-glycoprotein. *J. Pharmacol. Exp. Ther.* **293**, 376–82 (2000).

[49] Choo, E. *et al.* Pharmacological inhibition of P-glycoprotein transport enhances the distribution of HIV-1 protease inhibitors into brain and testes. *Drug Metab. Disp.* **28**, 655–660 (2000).

[50] Kandel, E., Jessell, T. & Schwartz, J. *Principles of Neural Science* (McGraw-Hill Companies, Inc., New York, 2000).

[51] Kurnik, D. *et al.* Tariquidar, a selective P-glycoprotein inhibitor, does not potentiate loperamide's opioid brain effects in humans despite full inhibition of lymphocyte P-glycoprotein. *Anesthesiology* **109**, 1092–9 (2008).

[52] Löscher, W. & Potschka, H. Drug resistance in brain diseases and the role of drug efflux transporters. *Nat. Rev. Neurosci.* **6**, 591–602 (2005).

[53] Löscher, W. Drug transporters in the epileptic brain. *Epilepsia* **48 Suppl 1**, 8–13 (2007).

[54] Bauer, B. *et al.* Seizure-induced up-regulation of P-glycoprotein at the blood-brain barrier through glutamate and cyclooxygenase-2 signaling. *Mol. Pharmacol.* **73**, 1444–53 (2008).

[55] Cirrito, J. *et al.* P-glycoprotein deficiency at the blood-brain barrier increases amyloid-β deposition in an Alzheimer disease mouse model. *J. Clin. Invest.* **115**, 3285–3290 (2005).

[56] Vogelgesang, S. *et al.* The role of P-glycoprotein in cerebral amyloid angiopathy; implications for the early pathogenesis of Alzheimer's disease. *Curr. Alzheimer Res.* **1**, 121–125 (2004).

[57] Vogelgesang, S. *et al.* Deposition of Alzheimer's B-amyloid is inversely correlated with P-glycoprotein expression in the brains of elderly non- demented humans. *Pharmacogenetics* **12**, 535–541 (2002).

[58] Phelps, M. *PET: Molecular Imaging and its Biological Applications* (Springer, New York, 2004).

[59] Innis, R. *et al.* Consensus nomenclature for in vivo imaging of reversibly binding radioligands. *J. Cereb. Blood Flow Metab.* **27**, 1533–9 (2007).

[60] Kawamura, K. *et al.* Synthesis and evaluation of [^{11}C]XR9576 to assess the function of drug efflux transporters using PET. *Ann. Nucl. Med.* **24**, 403–12 (2010).

[61] Kawamura, K. *et al.* Synthesis and in vivo evaluation of [^{18}F]fluoroethyl GF120918 and XR9576 as positron emission tomography probes for assessing the function of drug efflux transporters. *Bioorg. Med. Chem.* **19**, 861–70 (2011).

[62] Bauer, F. *et al.* Synthesis and in vivo evaluation of [^{11}C]tariquidar, a positron emission tomography radiotracer based on a third-generation P-glycoprotein inhibitor. *Bioorg. Med. Chem.* **18**, 5489–97 (2010).

[63] Dörner, B. *et al.* Synthesis and small-animal positron emission tomography evaluation of [^{11}C]elacridar as a radiotracer to assess the distribution of P-glycoprotein at the blood-brain barrier. *J. Med. Chem* **52**, 6073–6082 (2009).

[64] Lazarova, N. *et al.* Synthesis and evaluation of [*N*-methyl-^{11}C]*N-desmethyl*-loperamide as a new and improved PET radiotracer for imaging P-gp function. *J. Med.* **51**, 6034–43 (2008).

[65] Syvänen, S. *et al.* Duration and degree of cyclosporin induced P-glycoprotein inhibition in the rat blood-brain barrier can be studied with PET. *NeuroImage* **32**, 1134–41 (2006).

[66] Bankstahl, J. *et al.* Tariquidar-induced P-glycoprotein inhibition at the rat blood-brain barrier studied with (*R*)-^{11}C-verapamil and PET. *J. Nucl. Med.* **49**, 1328–35 (2008).

[67] Liow, J. *et al.* P-glycoprotein function at the blood-brain barrier imaged in monkey with [^{11}C]*N-desmethyl*-loperamide. *J. Nucl. Med.* **50**, 108–115 (2009).

[68] Piwnica-Worms, D., Kesarwala, A., Pichler, A., Prior, J. & Sharma, V. Single photon emission computed tomography and positron emission tomography imaging of multi-drug resistant P-glycoprotein–monitoring a transport activity important in cancer, blood-brain barrier function and Alzheimer's disease. *Neuroimag. Clin. N. Am.* **16**, 575–89, viii (2006).

[69] Zoghbi, S. *et al.* [^{11}C]Loperamide and its *N-desmethyl* radiometabolite are avid substrates for brain permeability-glycoprotein efflux. *J. Nucl. Med.* **49**, 649–56 (2008).

[70] Shetty, H. *et al.* Radiodefluorination of 3-Fluoro-5-(2-(2-[^{18}F](fluoromethyl)-thiazol-4-yl)ethynyl)benzonitrile ([^{18}F]SP203), a Radioligand for Imaging Brain Metabotropic Glutamate Subtype-5 Receptors with Positron Emission Tomography, Occurs by Glutathionylation in Rat B. *J. Pharmacol. Exp. Ther.* **327**, 727–725 (2009).

[71] Brown, A. *et al.* Metabotropic glutamate subtype 5 receptors are quantified in the human brain with a novel radioligand for PET. *J. Nucl. Med.* **49**, 2042–8 (2008).

[72] Lin, J. Transporter-mediated drug interactions: clinical implications and in vitro assessment. *Exp. Opin. Drug Metab. Toxicol.* **3**, 81–92 (2007).

[73] Huang, S., Temple, R., Throckmorton, D. & Lesko, L. Drug interaction studies: study design, data analysis, and implications for dosing and labeling. *Clin. Pharmacol. Ther.* **81**, 298–304 (2007).

[74] Wu, C. *et al.* Evidence for dual mode of action of a thiosemicarbazone, NSC73306: a potent substrate of the multidrug resistance linked ABCG2 transporter. *Mol. Cancer Ther.* **6**, 3287–96 (2007).

[75] Robey, R. *et al.* Pheophorbide a is a specific probe for ABCG2 function and inhibition. *Cancer Res.* **64**, 1242–1246 (2004).

[76] Liu, Z. *et al.* BIBW22 BS, potent multidrug resistance-reversing agent, binds directly to P-glycoprotein and accumulates in drug-resistant cells. *Molec. Pharmacol.* **50**, 482–492 (1996).

[77] Elsinga, P., Hendrikse, N., Bart, J., Vaalburg, W. & van Waarde, A. PET Studies on P-glycoprotein function in the blood-brain barrier: how it affects uptake and binding of drugs within the CNS. *Curr. Pharm. Des.* **10**, 1493–503 (2004).

[78] Hendrikse, N. *et al.* Complete in vivo reversal of P-glycoprotein pump function in the blood-brain barrier visualized with positron emission tomography. *Br. J. Pharmacol.* **124**, 1413–8 (1998).

[79] Levchenko, A. *et al.* Evaluation of 11C-colchicine for PET imaging of multiple drug resistance. *J. Nucl. Med.* **41**, 493–501 (2000).

[80] Elsinga, P. *et al.* Carbon-11-labeled daunorubicin and verapamil for probing P-glycoprotein in tumors with PET. *J. Nucl. Med.* **37**, 1571–1575 (1996).

[81] Del Vecchio, S., Zannetti, A., Aloj, L. & Salvatore, M. MIBI as prognostic factor in breast cancer. *Q. J. Nucl. Med.* **47**, 46–50 (2003).

[82] Chen, W. *et al.* Effects of MDR1 and MDR2 P-glycoproteins, MRP1, and BCRP / MXR / ABCP on the transport of [^{99m}Tc]tetrofosmin. *Biochem. Pharmacol.* **60**, 413– 426 (2000).

[83] Langer, O. *et al.* Pharmacoresistance in epilepsy: a pilot PET study with the P-glycoprotein substrate *R*-[^{11}C]verapamil. *Epilepsia* **48**, 1774–84 (2007).

[84] Ikoma, Y. *et al.* Quantitative analysis of [^{11}C]verapamil transfer at the human blood-brain barrier for evaluation of P-glycoprotein function. *J. Nucl. Med.* **47**, 1531–7 (2006).

[85] Lubberink, M. *et al.* Evaluation of tracer kinetic models for quantification of P-glycoprotein function using *R*-[^{11}C]verapamil and PET. *J. Cereb. Blood Flow Metab.* **27**, 424–33 (2007).

[86] Germann, U., Ford, P., Shlyakhter, D., Mason, V. & Harding, M. Chemosensitization and drug accumulation effects of VX-710, verapamil, cyclosporin A, MS-209 and GF120918 in multidrug resistant HL60/ADR cells expressing the multidrug resistance-associated protein MRP. *Anticancer Drugs* **8**, 141–155 (1997).

[87] Seneca, N. *et al.* Human brain imaging and radiation a PET radiotracer to measure the function of P-glycoprotein. *J. Nucl. Med.* **50**, 807–813 (2009).

[88] Kreisl, W. *et al.* P-glycoprotein function at the blood-brain barrier in humans can be quantified with the substrate radiotracer [^{11}C]*N-desmethyl*-loperamide. *J. Nucl. Med.* **51**, 559–66 (2010).

[89] Ferry, D., Russell, M., Kerr, D., Correa, I. & Prakash, S. [^{3}H]-GG918 (GF120918) binds with positive co-operativity to human P-glycoprotein with a nM dissociation constant. In *Proc. Am. Assoc. Cancer Res.*, 2246 (1996).

[90] Hyafil, F., Vergely, C., Vignaud, P. & Grand-perret, T. In vitro and in vivo reversal of multidrug resistance by in vitro and in vivo reversal of multidrug resistance by GF120918 , an acridonecarboxamide derivative. *Cancer Res.* **53**, 4595–4602 (1993).

[91] Kawamura, K. *et al.* Evaluation of limiting brain penetration related to P-glycoprotein and breast cancer resistance protein using [^{11}C]GF120918 by PET in mice. *Molec. Imaging Biol.* **13**, 152–60 (2011).

[92] de Bruin, M., Miyake, K., Litman, T., Robey, R. & Bates, S. Reversal of resistance by GF120918 in cell lines expressing the ABC half-transporter, MXR. *Cancer Lett.* **146**, 117–26 (1999).

[93] Stewart, A. *et al.* Phase I trial of XR9576 in healthy volunteers demonstrates modulation of P-glycoprotein in CD56+ lymphocytes after oral and intravenous administration. *Clin. Cancer Res.* **6**, 4186–91 (2000).

[94] Fox, E. & Bates, S. Tariquidar (XR9576): a P-glycoprotein drug efflux pump inhibitor. *Exp. Rev. Anticancer Ther.* **7**, 447–459 (2007).

[95] Shen, D. *et al.* Multiple drug-resistant human KB carcinoma cells independently selected for high-level resistance to colchicine, adriamycin, or vinblastine show changes in expression of specific proteins. *J. Biol. Chem.* **261**, 7762–70 (1986).

[96] Schneider, E., Horton, J., Yang, C., Nakagawa, M. & Cowan, K. Multidrug resistance-associated protein gene overexpression and reduced drug sensitivity of topoisomerase II in a human breast carcinoma MCF7 cell line selected for etoposide resistance. *Cancer Res.* **54**, 152–8 (1994).

[97] Henrich, C. *et al.* New inhibitors of ABCG2 identified by high-throughput screening. *Molec. Cancer Ther.* **6**, 3271–8 (2007).

[98] Hall, M. *et al.* Synthesis and structure-activity evaluation of isatin-β-thiosemicarbazones with improved selective activity toward multidrug-resistant cells expressing P-glycoprotein. *J. Med. Chem.* **54**, 5878–89 (2011).

[99] Lee, C. *et al.* HIV-1 protease inhibitors are substrates for the MDR1 multidrug transporter. *Biochemistry* **37**, 3594–601 (1998).

[100] Hall, H., Halldin, C., Farde, L. & Sedvall, G. Whole hemisphere autoradiography of the postmortem human brain. *Nucl. Med. Biol.* **25**, 715–9 (1998).

[101] Yoshimori, T., Yamamoto, A., Moriyama, Y., Futai, M. & Tashiro, Y. Bafilomycin A1, a specific inhibitor of vacuolar-type H(+)-ATPase, inhibits acidification and protein degradation in lysosomes of cultured cells. *J. Biol. Chem.* **266**, 17707–12 (1991).

[102] Altan, N., Chen, Y., Schindler, M. & Simon, S. Tamoxifen inhibits acidification in cells independent of the estrogen receptor. *Proc. Natl. Acad. Sci. U.S.A* **96**, 4432–7 (1999).

[103] Agostinelli, E. & Seiler, N. Lysosomotropic compounds and spermine enzymatic oxidation products in cancer therapy (review). *Int. J. Oncol.* **31**, 473–84 (2007).

[104] Feng, B. *et al.* In vitro P-glycoprotein assays to predict the in vivo interactions of P-glycoprotein with drugs in the central nervous system. *Drug Metab. Disp.* **36**, 268–275 (2008).

[105] Shukla, S., Robey, R., Bates, S. & Ambudkar, S. The calcium channel blockers, 1, 4-dihydropyridines, are substrates of the multidrug resistance-linked ABC drug transporter, ABCG2. *Biochemistry* **45**, 8940–8951 (2006).

[106] Clark, J. *et al.* Guide for the Care and Use of Laboratory Animals. Tech. Rep., National Academy Press, Washington, DC (1996).

[107] Löscher, W. & Potschka, H. Blood-brain barrier active efflux transporters: ATP-binding cassette gene family. *NeuroRx* **2**, 86–98 (2005).

[108] Schindler, M., Grabski, S., Hoff, E. & Simon, S. Defective pH regulation of acidic compartments in human breast cancer cells (MCF-7) is normalized in adriamycin-resistant cells (MCF-7adr). *Biochemistry* **35**, 2811–17 (1996).

[109] Willingham, M., Cornwell, M., Cardarelli, C., Gottesman, M. & Pastan, I. Single cell analysis of daunomycin uptake and efflux in multidrug-resistant and -sensitive KB cells: effects of verapamil and other drugs. *Cancer Res.* **46**, 5941–6 (1986).

[110] Moriyama, Y., Manabe, T., Yoshimori, T., Tashiro, Y. & Futai, M. ATP-dependent uptake of anti-neoplastic agents by acidic organelles. *J. Biochem.* **115**, 213–8 (1994).

[111] Koponen, M., Grieder, A., Hauser, R. & Loor, F. Interference of cyclosporin with lymphocyte proliferation: effects on mitochondria and lysosomes of cyclosporin-sensitive or -resistant cell clones. *Cell Immunol.* **93**, 486–96 (1985).

[112] Millot, C., Millot, J., Morjani, H., Desplaces, A. & Manfait, M. Characterization of acidic vesicles in multidrug-resistant and sensitive cancer cells by acridine orange staining and confocal microspectrofluorometry. *J. Histochem. Cytochem.* **45**, 1255–64 (1997).

[113] Dohse, M. *et al.* Comparison of ATP-binding cassette transporter interactions with the tyrosine kinase inhibitors imatinib, nilotinib, and dasatinib. *Drug Metab. Disp.* **38**, 1371–1380 (2010).

[114] Choo, E. *et al.* Differential in vivo sensitivity to inhibition of P-glycoprotein located in lymphocytes, testes, and the blood-brain barrier. *J. Pharmacol. Exp. Ther.* **317**, 1012–1018 (2006).

[115] Kamiie, J. *et al.* Quantitative atlas of membrane transporter proteins: development and application of a highly sensitive simultaneous LC/MS/MS method combined with novel in-silico peptide selection criteria. *Pharm. Res.* **25**, 1469–1483 (2008).

[116] Pardridge, W. Blood-brain barrier biology and methodology. *J. Neurovirol.* **5**, 556–69 (1999).

[117] Halldin, C., Gulyas, B., Langer, O. & Farde, L. Brain radioligands – state of the art and new trends. *Q. J. Nucl. Med.* **45**, 139–52 (2001).

[118] Uchida, Y. *et al.* Quantitative targeted absolute proteomics of human blood-brain barrier transporters and receptors. *J. Neurochem.* **117**, 333–345 (2011).

[119] Sasongko, L. *et al.* Imaging P-glycoprotein transport activity at the human blood-brain barrier with positron emission tomography. *Clin. Pharmacol. Ther.* **77**, 503–14 (2005).

[120] Piwnica-Worms, D. & Sharma, V. Probing multidrug resistance P-glycoprotein transporter activity with SPECT radiopharmaceuticals. *Curr. Top. Med. Chem* **10**, 1834–45 (2010).

[121] Sharma, V., Prior, J., Belinsky, M., Kruh, G. & Piwnica-Worms, D. Radiopharmaceutical for SPECT and PET of MDR1 P-glycoprotein transport activity in vivo: validation in multidrug-resistant tumors and at the blood–brain barrier. *J. Nucl. Med.* **46**, 354–364 (2005).

[122] Waarde, A. *et al.* Synthesis and preclinical evaluation of novel PET probes for P-glycoprotein gunction and expression. *J. Med. Chem* **52**, 4524–4532 (2009).

[123] Tournier, N. *et al.* Transport of selected PET radiotracers by human P-glycoprotein (ABCB1) and breast cancer resistance protein (ABCG2): an in vitro screening. *J. Nucl. Med.* **52**, 415–23 (2011).

[124] Mairinger, S. *et al.* Synthesis and in vivo evaluation of the putative breast cancer resistance protein inhibitor [^{11}C]methyl 4-((4-(2-(6,7-dimethoxy-1,2,3,4-tetrahydroisoquinolin-2-yl)ethyl)phenyl)amino-carbonyl)-2-(quinoline-2- carbonylamino)benzoate. *Nucl. Med. Biol.* **37**, 637–644 (2010).

[125] Okamura, T., Kikuchi, T. & Irie, T. PET imaging of MRP1 function in the living brain: method development and future perspectives. *Curr. Top. Med. Chem* **10**, 1810–1819 (2010).